Multiple Model Adaptive Regulation

A Thesis

Submitted to the Faculty

of

Drexel University

by

Eric Dean Peterson

in partial fulfillment of the

requirements for the degree

of

Doctor Of Philosophy in Mechanical Engineering

November 2014

Table of Contents

List of Tables

List of Figures

Abstract

Multiple Model Adaptive Regulation

Eric Dean Peterson

Advisor: Harry Kwatny, PhD

A single controller may be inadequate for systems that experience structural changes that arise, for example, from component failures. Such systems are often modeled by a family of plants with structural diversity. At any given time the appropriate plant model is uncertain. Adaptation is required for the parameter dependent family of plants but continuous adaptive regulation is limited by relative degree and right half plane zeros. A form of adaptive regulation is presented that accommodates these changes.

The Multiple Model Adaptive Regulator selects a controller from a predefined set to achieve performance goals. In general, the set of controllers is finite although the family of plants may be continuous. The set of controllers accommodates a structurally diverse family of plants. A multiple model controller design has two subproblems, covering and switching. The covering subproblem is to design a small set of controllers such that each possible plant is stabilized by at least one controller. The switching subproblem is to select a stabilizing controller from the set of controllers. In this research, the covering and switching subproblems are solved with LQR state feedback and Lyapunov function switch logic respectively. The LQR and Common Quadratic Lyapunov Function design problems are combined into a set of Linear Matrix Inequalities (LMI) and concurrently solved. Design constraints on the open loop plant and the regulator are presented. The multiple model adaptive regulator is applied to systems with diverse zero structure.

1. INTRODUCTION

1.1 Motivation

The importance of the open loop zero structure for closed loop regulation has long been known, c.f. [KS72, Fra77, KBB91]. In fact, an upper bound on *simultaneous regulation* of plants as a function of zero structure is known [BK94]. Consider a parameter-dependent family of plants partitioned into subfamilies with equivalent zero structure. The partitions consist of points in the parameter space that do not satisfy the open loop existence conditions for regulator design. Points that fail the existence condition may be called singular points. As shown in [KBB91], singular points form codimension-1 submanifolds that partition the parameter space into disjoint subfamilies. A regulator designed for one subfamily will generically fail to regulate a plant in a different subfamily [BK94]. This bound on *simultaneous regulation* of subfamilies motivates the novel multiple model adaptive control design technique presented here.

Multiple model adaptive techniques have been proposed to accommodate systems with diverse dynamics [ABDB$^+$00, AM02, Bos08]. Multiple model adaptation selects a controller from a predefined set. In general, the set of controllers is finite although the family of plants may be continuous. Multiple model adaptive control design presents two subproblems, covering and switching.

The design of a finite set of controllers to guarantee stability across the family of plants, called the *covering problem*, is fundamental. Several authors have considered covering from the perspective of controller robustness, [ABDB$^+$00, Bos08]. These designs start with a finite set of plant models and employ robustness metrics to cover the family of plants. We propose a covering method that starts with plant subfamilies and obtains controllers for convex regions of the subfamily's parameter space. This covering method accommodates singular surfaces in the parameter space.

The design of switch logic to select a stabilizing controller from the set of controllers is the second fundamental problem of multi-model adaptive control. The design method proposed here unifies switch logic and control covering into a single computation. Recall that a single algebraic Riccati equation (ARE) obtains a quadratic Lyapunov function matrix and linear quadratic regulator (LQR) gains. And the quadratic ARE can be written as a convex linear matrix inequality (LMI) to facilitate fast solution. A set of algebraic Riccati inequalities for a convex region of the subfamily's parameter space may be solved for a common LQR state feedback gain and a common quadratic Lyapunov function (CQLF). By choosing Lyapunov function based switch logic and LQR control gains, the multi-model covering and switch logic design computations are unified into a set of LMIs.

A formal statement of the problem solved herein for linear systems is provided next. The problem statement for nonlinear systems is summarized here and detailed in Chapter 7. The introductory section ends with a literature survey and outline.

1.2 Problem Statement

Define a parameter dependent family of linear plants

$$\begin{aligned} \dot{x} &= A(\theta)\, x + B(\theta)\, u \\ e &= C(\theta)\, x \end{aligned} \tag{1.1}$$

as $\mathbf{p}(\theta) \in \mathcal{P}$ where $u \in R^m$, $x \in R^n$, $e \in R^p$. The parameter dependent matrices are $A(\theta)$, $B(\theta)$, $C(\theta)$ where $\theta \in R^k$ is a vector of unknown but bounded constant parameters.

Shorthand notation for the parameter dependent matrices $A_\theta \equiv A(\theta)$, etc. will also be used. The goal is to regulate the plant with respect to a set of exogenous signals generated by the model

$$\dot{\vartheta} = Z\vartheta \tag{1.2}$$

where $\vartheta \in R^r$. The set of exogenous signals considered in this thesis is comprised of step commands and constant disturbances such that $Z = 0_r$. The exogenous signals drive the

plant (1.1) through matrices E and F in the following manner

$$\begin{aligned} \dot{x} &= A(\theta)\, x + B(\theta)\, u + E\vartheta \\ \dot{\vartheta} &= Z\vartheta \\ e &= C(\theta)\, x + F\vartheta \end{aligned} \tag{1.3}$$

As is well known, such disturbance models can effectively characterize command signals and disturbances. The problem of designing robust regulators for systems described by (1.3) is well studied, e.g., [Dav72, Fra77, KK78]. In this work an *adaptive* regulator is sought that associates an appropriate robust regulator with the actual occurring member of the plant family. The two central problems in doing this are:

- *Covering Problem*: Given a range of plant parameters θ, design a set of controllers $\mathcal{C}$ such that each $\mathbf{p}(\theta) \in \mathcal{P}$ is stabilized by at least one $C_i \in \mathcal{C}$.
- *Switch Logic Design*: Given a plant family $\mathcal{P}$ and a finite control covering, design a switching logic that guarantees convergence to a stabilizing regulator for the actual occurring plant.

The next three chapters apply multiple model adaptive control to linear parameter varying systems (1.1) with diverse zero structure. While parameter bounds are known a priori, the actual occurring or "true" parameter value is not known. A parameter value may change due to a fault for example. Parameter dependent nonlinear systems are considered in later chapters. The following section highlights differences in the regulation of parameter dependent linear and nonlinear systems.

1.2.1 Nonlinear Problem Statement

A more general form of (1.1) is the nonlinear parameter dependent system

$$\begin{aligned} \dot{x} &= f(x, u, \vartheta) \\ e &= h(x, \vartheta) \end{aligned} \tag{1.4}$$

where the vector of unknown but bounded parameters $\vartheta \in R^k$ act as state disturbances or reference inputs. The ϑ belong to a known class of signals generated by the linear system (1.2). The nonlinear parameter dependent system is different from the linear parameter dependent system in several ways.

A detailed example of MMAR for nonlinear systems Eqn. (1.4) is given in Chapter 7.

Parameter Dependence

In contrast to the parameter dependent linear system Eqn. (1.3), the parameters θ and ϑ are combined into a single parameter ϑ in the parameter dependent nonlinear system Eqn. (1.4). Distinguishing between parametric modeling error (θ) and exosystem states (ϑ) is advantageous for the linear case. When $Z = 0_r$ the constant parameters θ and ϑ in Eqn. (1.3) have a very different impact on the output error convergence as shown in the following example.

Example 1.1. *The following example illustrates the difference in behavior of parameters θ and ϑ in linear and nonlinear systems.*

Linear Systems *Consider the Single Input Single Output (SISO) linear system with scalar exogenous inputs shown in Fig. 1.1. The error $e = y_{ref} - y$ as a function of the*

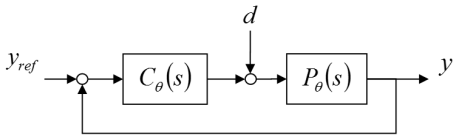

Figure 1.1: Single Input Single Output Feedback System

reference input $y_{ref}(s)$ *and the disturbance* $d(s)$ *is*

$$e(s) = y_{ref}(s) - y(s) = \frac{1}{1 + P_\theta(s) C_\theta(s)} \begin{bmatrix} 1 & -P_\theta(s) \end{bmatrix} \begin{bmatrix} y_{ref}(s) \\ d(s) \end{bmatrix} \tag{1.5}$$

Where $P_\theta(s)$ *and* $C_\theta(s)$ *depend on* θ*. The exogenous signal vector*

$$\vartheta(s) = \begin{bmatrix} y_{ref}(s) \\ d(s) \end{bmatrix}$$

generated by a linear system Eqn. (1.2) does not depend on θ*. The magnitude of the error* $e(s)$ *of Eqn. (1.5) is linear in* $\vartheta(s)$ *and the rate of convergence of* $e(s)$ *is independent of* $\vartheta(s)$*. Hence stable regulation is independent of* ϑ *for linear systems.*

Nonlinear Systems *Consider a scalar affine nonlinear system*

$$\dot{x} = f(x) + g(x, \theta) u + \vartheta$$

where θ *is an unknown parameter and* ϑ *is an exogenous disturbance. Assume constant state feedback* $u = k(x)$*. An equilibrium state* x^* *is a solution of the implicit function* $\mathcal{X} : R^{k+r} \to R^n$

$$0 = f(x^*) + g(x^*, \theta) k(x) + \vartheta$$

where $x^* = \mathcal{X}(\theta, \vartheta)$ *is a function of* θ *and* ϑ*. Since* x^* *depends on* ϑ*, the input map* $g(\mathcal{X}(\theta, \vartheta), \theta)$ *depends on* ϑ*. Consider distinct disturbances* $\vartheta^\circ \neq \vartheta^\diamond$ *with distinct equilibrium points* $x^\circ = \mathcal{X}(\theta, \vartheta^\circ)$ *and* $x^\diamond = \mathcal{X}(\theta, \vartheta^\diamond)$*. If the input map changes sign such that* $sign\, g(x^\circ, \theta) \neq sign\, g(x^\diamond, \theta)$ *but the state feedback sign is unchanged*

sign k $(x^{\circ}) =$ *sign k* $(x^{\diamond})$*, then stability may be lost at that equilibrium. For example if*

$$\begin{aligned} f(x) &= 0 \\ g(x,\theta) &= Sign(x) \\ k(x) &= -x \end{aligned}$$

then a stable equilibrium exists for all $\vartheta > 0$*. But no equilibrium exists for* $\dot{x} = \vartheta - |x|$ *when* $\vartheta < 0$ *(*$|\cdot|$ *is absolute value). In this simple example stability is related to translation of the equilibrium state.*

In general, a robust regulator applied to a nonlinear system may fail due to perturbation of ϑ. Thus, a distinction between θ and ϑ is superfluous when the underlying system is nonlinear, and all parameters are labeled exogenous inputs (ϑ).

The robust regulation method developed in this thesis is applied to a linear family of plants derived from a nonlinear system in Chapter 7. For more information on regulation for nonlinear systems, see Chapter 8 of [Isi95].

Convexity

The covering problem is solved in Sec. 3.1 for linear systems using convexity of the parameter dependent LMI. The LMI is linear in the parameter θ and can be used to solve the quadratic LQR problem. Unfortunately the parameter dependent nonlinear system Eqn. (1.4) is neither linear nor convex in ϑ. Covering for nonlinear systems is discussed in Chapter 7.

1.3 Literature Survey

Development of Multiple Model Adaptive Control (MMAC) is surveyed followed by two examples of recent MMAC implementations.

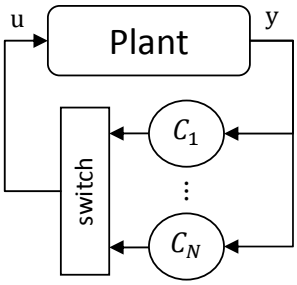

Figure 1.2: Multiple Model Adaptive Control (MMAC)

1.3.1 Multiple Model Adaptive Control

Controller Structure

The generic multiple model control structure is illustrated in Fig. 1.2. Each controller C_i regulates some region of $\mathcal{P}$ and the set of controllers $\mathcal{C} = \{C_i\}$ is sufficiently large such that each possible plant $\mathbf{p}(\theta) \in \mathcal{P}$ is regulated by at least one C_i. Hence the two key design problems consist of finding the set $\{C_i\}$ and implementing a switching strategy to choose a C_i to stabilize (or regulate) the actual occurring plant. Early work on MMAC primarily focused on the switch strategy whereas recent papers influenced by robust control ideas consider the covering problem.

This generic structure can support numerous control design methods for C_i, even within the same set $\mathcal{C}$. The switch is a supervisory system that monitors a performance signal and switches controllers as needed. In general the supervisor will contain one or more discrete states such that MMAC is a hybrid system. A hybrid system contains both continuous and discrete states.

History

Early papers on Multiple Model Adaptive Control implement a convex combination of tuned controllers scheduled by Kalman filter covariances [ACD$^+$77, MP89]. Recent work uses covariances from an Extended Kalman filter [DG08]. However, stability is not shown

in these papers.

A distinct line of research [Mår85, FB86, MP89] uses switching to bound the a priori information needed to design an adaptive system. For instance, the relative degree and high-frequency gain are two system invariants required for a priori design of a CDAC. These two properties, even if unknown, have a limited set of feasible combinations. Conceivably, a model for each combination could be designed and the true model then identified on-line. Martensson [Mår85] shows stability in the abstract by 'turning over every rock.' Likewise, Miller [MD89], however tenuous, shows exponential stability.

A form of MMAC which switches between parallel observers was introduced to avoid unstable parameter estimates [MGHM88]. This switching formulation underpins the work reviewed in this thesis. Morse and coworkers advance MMAC with hysteresis switching for stability in servo problems [MMG92, Mor96, HM99, HLSM$^+$01] and nonlinear systems [HLM03]. While early MMAC work used switching to ensure stability, later work (including the papers surveyed below) seeks performance improvement.

Alternatively, Narendra [NB94, NB97] proposes Multiple Models with Switching and Tuning (MMST) to improve the transient performance of continuous direct adaptive control. MMST focuses on finding the best possible initial conditions from which the standard CDAC algorithm will perform well. MMST allows arbitrarily fast switching, but retains the four CDAC constraints provided above. The parallel generation of parameter estimates or performance signals via observers is the unifying theme for many MMAC formulations including Narendra and Morse.

Morse seeks a unified theory of tunability [Mor90]. An open loop system is constructed by breaking the loop at the tuner. If this open loop system is not detectable, the process is not (weakly) tunable. A 'nontunable' example is provided; a priori knowledge of the high frequency gain sign is needed for tunability. Note that MMAC enables knowledge of the high frequency gain sign to be commuted outside the continuous adaptive controller. Instead of an a priori parameter constraint, the MMAC supervisor uses observed outputs

to detect an unbounded solution and then choose a different parameterized controller to stabilize the system. The system may not be detectable to the tuner but a finite number of unbounded solutions can be discarded using observed outputs. This is in the spirit of Martensson [Mår85].

Switching

Four examples of switch logic are illustrated in Fig. 1.3. The switch logic examples are discussed below.

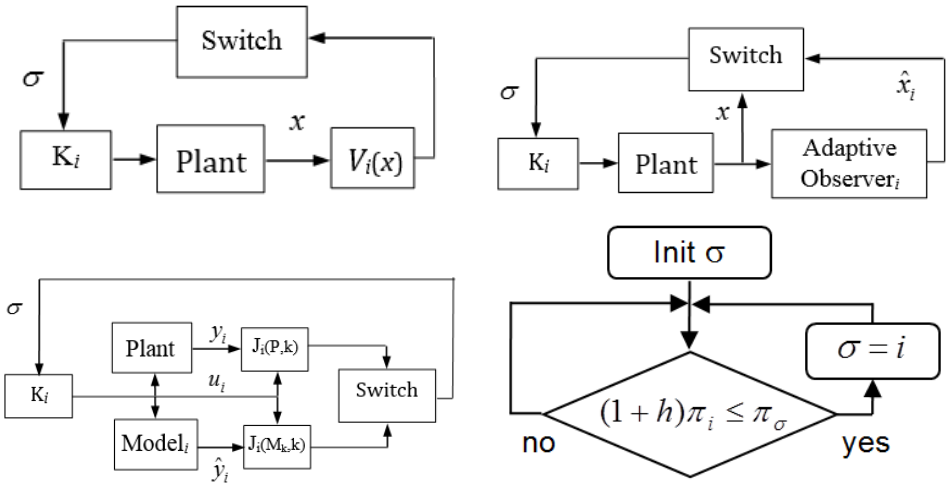

Figure 1.3: Switch Logic Strategies: (Top Left) Lyapunov Function [AM02]; (Top Right) Adaptive Observers [Bos08]; (Bottom Left) Normalized Quadratic Cost [MA01]; (Bottom Right) Hysteresis Switch Logic [HM99]

Lyapunov Based Switching [AM02] This switch logic is a form of falsification, or finding the correct controller by process of elimination. Each controller C_i has a corresponding Lyapunov function V_i. If controller σ is in the loop, then V_σ is tested for negative definite time rate of change. Only the "in the loop" controller is tested. In general the system may be nonlinear, but the states must be measurable. A "dwell time", or finite time on the

selected controller, is not required. The stability proof does not imply that switching stops on a tuned controller, only that the performance be better than some nominal rate of decay.

Adaptive Observers [Bos08] Boskovic, et. al. use a finite set of adaptive observers to identify a plant with unknown parameters. The states are assumed to be measurable and the observer output is compared with the true state. Adaptive observer parameters are updated with a gradient projection rule. The updated parameters are then feed back to the control laws for an indirect multiple model adaptive scheme, similar to [NB97]. The switch logic chooses the observer that minimizes the state estimation error $e_i = \hat{x}_i - x$.

Normalized Quadratic Cost Function [MA01] In the previous case, each Lyapunov function was tested for negative definiteness. In this case the 'best', or 'most nearly true' controller is chosen based on a normalized quadratic cost function of control inputs and plant outputs. The cost for the *true* plant model with controller K_i is $J(M^*, K_i)$. The cost for model M_j with controller K_i is $J(M_j, K_i)$. The switch criteria is the percent difference of the cost of the true plant model M^* and model M_j while using the controller K_i, i.e. $\arg\min_i \frac{J(M^*, K_i) - J(M_j, K_i)}{J(M_j, K_i)}$. The normalization is needed since the cost $J(\cdot, K_i)$ may vary for model M_j. Since only one plant/controller pair can be in operation at one time, the inference problem is approximated by filtering. This selection of the 'best' controller is superficially more desirable than the "test and discard" Lyapunov method above. The seminal value of this paper is the recognition that selection based on output estimation will be disproportionately weighted to high frequency content. The normalization requirement motives a filter design to weight the frequency band of interest.

Hysteresis Switch Logic [HM99] Only the switch logic is diagrammed in Fig. 1.3. The system diagram is similar to the Adaptive Observer method but with fixed observers with output y_i instead of x_i. The performance signals π_i are formed from low pass filtering e_i^2 where error $e_i = \hat{y}_i - y$. The states are assumed unavailable for measurement. The switch

logic works as follows:

1. Find the index of the smallest performance signal $q = \arg\min_i \pi_i$
2. If $(1 + h)\,\pi_q \leq \pi_\sigma$, then switch on control with index q.

The hysteresis switch logic is related to an average dwell time. An exponential stability margin is obtained by adjusting h, the hysteresis coefficient, to ensure the average dwell time introduced by the switch logic is greater than the system specific average dwell time. This work is a clever adaptation of the common dwell time switch logic for hybrid systems.

While much has been written about the switch logic of supervisory adaptive control, the design of component controllers has been left to traditional methods. Methods to coordinate the design of parallel estimators and controllers is an open problem. Preliminary quantitative stability results are presented in [PZ07]. Ensuring the stability of a family of controllers over the space of unknown plants is termed the covering problem.

Covering

Two examples of covering are surveyed in detail in the following section.

1.3.2 Recent MMAC implementations

Two previous multiple model adaptive regulation methods are examined: the ν-gap metric and a Lyapunov function based "Model Set Reduction" technique.

v-gap metric

For a known plant with 'small' parameter variations, robust control techniques ensure stable feedback control systems. Accordingly, the problem of choosing observer & controller pairs to infer & implement stable control over large parameter variations was first approached from the robust control framework [PK01, ABDB$^+$00]. In [ABDB$^+$00], the Vinnicombe 'v-gap' metric, a measure of the distance between plants, is used in place of

unstructured uncertainty. Implementation of the 'v-gap' metric may be summarized as follows:

1. Obtain the infinity norm of the internal stability transfer function matrix (factored as in [ZDG$^+$96], Lemma 18.4)

$$T(P,C) = \left\| \begin{bmatrix} I \\ C \end{bmatrix} \cdot (I - PC)^{-1} \cdot \begin{bmatrix} P & I \end{bmatrix} \right\|_\infty$$

2. Obtain the infinity norm of the v-gap metric

$$\delta_v(P, P_\theta) = \left\| (I + P_\theta P_\theta^*)^{-\frac{1}{2}} (P_\theta - P) (I + PP^*)^{-\frac{1}{2}} \right\|_\infty$$

3. Apply the small gain theorem to the product of steps 1. and 2.,

$$T(P,C) \cdot \delta_v(P, P_\theta) < 1 \Rightarrow \text{Stability}$$

4. Moreover, this bound is tight since

$$T(P,C) \cdot \delta_v(P, P_\theta) \geq 1 \Rightarrow \text{Instability}$$

This method may be very conservative and does not maintain the structure of the parameter uncertainty of the state space model.

Model Set Reduction

A method to guarantee covering of parameter dependent state space representations is proposed in [PBKG08]. Stability of systems with general linear compensators (i.e. observer + state feedback) is ensured through a "grid and check" method. This method works by solving the algebraic Riccati equation (ARE) for a nominal system and then ensuring

Lyapunov stability for a perturbed system. Assume additive noise Θ such that

$$A + BK - \Theta$$

where the perturbed dynamics are Lyapunov stable if

$$\begin{aligned} (A_{cl} - \Theta)^T P + P(A_{cl} - \Theta) + Q &< 0 \\ A_{cl}^T P + P A_{cl} &< -Q + \Theta^T P + P\Theta \\ A_{cl}^T P + P A_{cl} &< -Q + 2\|P\|_2 \|\Theta\|_2 \end{aligned}$$

where $A_{cl} = A + BK$ and the design weight $Q > 0$. Lyapunov stability implies a bound on Θ, i.e.

$$A_{cl}^T P + P A_{cl} < 0 \quad \Rightarrow \quad 2\|P\|_2 \|\Theta\|_2 < \|Q\|_2 \tag{1.6}$$

The steps for evaluating stability at a nominal parameter value are

1. Solve for a state feedback K and matrix P that satisfies the Lyapunov equation

$$A_{cl}^T P + P A_{cl} + Q < 0 \tag{1.7}$$

2. Obtain bound ϱ on $\|\Theta\|_2$

$$\|\Theta\|_2 \leq \varrho < \frac{\|Q\|_2}{2\|P\|_2} \tag{1.8}$$

3. Place surrounding grid points within the bound $\|\Theta\|_2 \leq \varrho$. Move to adjacent grid point and repeat these three steps.

Notice a termination condition is not provided. If $\dim \Theta > 1$ the covering consists of overlapping spheres. In [PBKG08] covering is checked with stochastic methods. Verification that the union of a set of spheres contain a subspace is a nontrivial problem in general.

The grid is refined by sequential application of Steps 1-3. Each point in the parameter space must be within a distance ϱ from a stabilizing controller. The grid of parameter

space points used for controller design is refined (i.e. additional points per unit subspace) to satisfy the bound ϱ on the norm of additive error.

Two drawbacks are evident:

- This method may suffer from extreme conservatism due to the brute force application of matrix norms.
- Whereas the frequency domain v-gap method is invariant to similarity transformations, conservatism of this method depends on the state space representation.

Observe that the quadratic Lyapunov function Eqn. (1.7) can be written as an LMI which is linear and hence convex in parameter variation. This observation can relax the conservatism of Eqn. (1.8) and is fundamental to the MMAR method presented here.

1.4 Thesis Organization & Contribution

1.4.1 Organization

This paper is organized as follows:

- Section 2 summarizes the regulation problem and details the relationship between zero dynamics and simultaneous regulation.
- Section 3 presents our concept of multiple model adaptive regulation (MMAR).
- Section 4 our main results, details MMAR.
- Section 5 analyzes the motivating example, parameter dependent aircraft dynamics.
- Section 6 design details for an idealized system
- Section 7 design details for four state longitudinal aircraft dynamics.

1.4.2 Contributions

The contributions of the thesis are listed below.

1. Unification of control covering and switch logic design. Whereas previous multiple model adaptive control (MMAC) systems obtain the controller and switch logic separately through trial-and-error, the MMAC system presented in this thesis unifies the control and switching subproblems. The covering and switching subproblems are solved with Linear Quadratic Regulator (LQR) state feedback and Common Quadratic Lyapunov Function (CQLF) switch logic respectively. This allows the control and switch subproblems to be combined into a set of Linear Matrix Inequalities (LMI) and concurrently solved. This unification into LMIs facilitates design automation since the set of LMIs can be solved quickly and efficiently in a single computation.

2. A convex parameter space covering technique for MMAC system design. A (quadratic) Lyapunov function for a linear system with linear uncertainty is quadratic in the state dynamics and thus quadratic in the linear uncertainty. Previous adaptive and multiple model systems employ a Lyapunov function to bound the linear uncertainty, but the quadratic dependence on the parametric uncertainty leads to conservative stability estimates via the small gain theorem. By expressing Lyapunov functions with parametric uncertainty as LMIs, stability is expressed as linear inequalities with parametric uncertainty. This observation on the expression of parametric uncertainty is combined with the quadratic design techniques above (LQR & CQLF) to improve control covering computation as follows:

   (a) Parameter space may be "covered" with convex polytopes. Designing a set of controllers such that any region of the parameter space is covered by at least one controller is simplified by the use of convex polytopes of the designer's choice. In contrast, verification of control covering for a robust control design with spherical stability regions is difficult. Convex polytopes accommodate the abrupt bounds

on simultaneous regulation of systems with diverse zero structure.

(b) Computational efficiency and accuracy of the convex covering. Only the vertices of the closed convex polytopes need to be checked for stability. Conservatism is not introduced in contrast to stability verification via the small gain theorem.

3. Flexibility in designing a constant state feedback gain for a family of plants with convex parametric uncertainty is proved. Both the use of an LMI to solve the LQR problem and the use of multiple LMIs to solve for a CQLF are well known. The existence of a CQLF for the set of LQR inequalities implies the existence of a common state feedback gain K. But what is the range of K? More specifically, if a CQLF matrix P exists for a polytopic region of the parameter space and K takes the familiar form $K = -R^{-1}B(\theta)^T P$ where P and in general R are constant but $B(\theta)$ varies over the polytope, how much flexibility exists in choosing $B_* \in B(\theta)$ for a constant state feedback gain $K = -R^{-1}B_*^T P$? It is shown that any $B_* \in B(\theta)$ for all $B(\theta)$ in the polytope of plants is acceptable. However, some choices of B_* may require re-solving the ARE for an updated P. Guidance on the selection of B_* is provided. See Section 4.3.1 for details.

4. A restriction on the type of regulator synthesis is identified. A common robust regulation synthesis is the Disturbance Estimation regulator which obtains a compensator with observer subject to the internal model requirement. However, the LMI approach presented here is limited to Error Augmentation type regulators. The design of a CQLF for a Disturbance Estimation regulator subject to linear parametric uncertainty is shown to be a bilinear matrix inequality. See Section 4.4.2 for details.

5. Implementation of Lyapunov level set switch logic for robust regulation. Previous work with Lyapunov level set switch logic considers only stabilization (to the origin). But by design, robust regulation is unaffected by equilibrium position. However, Lyapunov function switch logic is affected by equilibrium position. To indicate convergence to

an equilibrium state, the Lyapunov function requires a priori knowledge of the system equilibria. Thus, arbitrary (nonzero) location of the equilibrium state for output regulation presents new challenges. Several methods to ameliorate the lack of a prori knowledge of the equilibrium state are presented.

2. REGULATION AND ZERO STRUCTURE

Before proceeding with adaptive regulation of the parameter dependent system defined in Eqn. (1.1) it is necessary to summarize some general results for the regulation of an individual linear system.

Output regulation of linear systems may be divided into subproblems in order of increasing generality:

- S*tabilization* of system output to a zero reference input such that the equilibrium state is the origin $x = 0$.
- S*et-point* regulation of system output to a step reference input such that the equilibrium state is a nonzero constant $x = c$.
- *Tracking* a dynamic reference such that the equilibrium state is a function of time $x = f(t)$.

Regulation in the presence of reference inputs and state disturbances may be solved concurrently. A precise definition of the regulation problem considered herein is given below.

The importance of zero structure for regulation is well known. Arbitrarily small changes in the zero structure may cause abrupt changes in the stability of linear regulators. Accommodating the effects of zero structure change on output regulation is the motivation for this thesis. This section defines linear regulation, details two synthesis methods, and describes the effect of zero structure change on linear regulators.

2.1 The Linear Regulator Problem

Consider a parameter independent linear system with disturbance state vector ϑ

$$\begin{aligned} \dot{x} &= Ax + Bu + E\vartheta \\ \dot{\vartheta} &= Z\vartheta \\ e &= Cx + F\vartheta \end{aligned} \tag{2.1}$$

It will be assumed that B and C are of full rank.

Definition 2.1. *Regulation requires both* $\lim_{t\to\infty} e(t) = 0$ *and internal stability. Regulation in the presence of variation in the plant matrices* A, B, *and perhaps* C *is known as* robust regulation *or* structurally stable regulation.

Structurally stable regulation uses error feedback and incorporates an internal model of the external signals to be tracked and disturbances to be rejected.

Definition 2.2. *Robust regulation requires an internal model of the exogenous signals. A matrix* M *incorporates an internal model of matrix* Z *if the minimal polynomial of* Z *divides at least* p *invariant factors of* M. *The invariant factors of* M, *related to elementary divisors, motivate the Smith canonical form. The minimal matrix polynomial* $\mathcal{M}(Z)$ *is the monic polynomial in* Z *of smallest degree* d *such that*

$$\mathcal{M}(Z) = \sum_{i=0}^{d} c_i Z^i = 0$$

For the case $Z = 0_k$, the minimal polynomial has degree one regardless of k. Hence, if $k > 0$, an internal model of dimension equal to or greater than the number of outputs (p) is sufficient for robust regulation. The regulator is robust to variation in the k parameters, the plant matrices, and the exogenous inputs when an internal model is included as in Eqn. (2.5).

Theorem 2.3. *The structurally stable linear regulator incorporates an internal model of* Z.

Proof. Theorem 2 of [FW75a] □

Note that the internal model must be controllable from the regulated outputs (e) and observable from the inputs (u).

Regulator design is contingent on properties of the open loop plant as follows:

Theorem 2.4. *[Fra77] Necessary and sufficient conditions for structurally stable regulation are*

1. (A, B) *stabilizable*
2. (C, A) *detectable*
3. *Rank* $\begin{bmatrix} \lambda_i - A & B \\ C & 0 \end{bmatrix} = n + r$ *for* λ_i *an eigenvalue of* Z

The third condition requires the plant transmission zeros to be different than the spectrum of Z. An alternate statement of the third condition that X, U exist such that

$$\begin{aligned} AX - XZ + BU &= E \\ CX \qquad\quad &= F \end{aligned} \tag{2.2}$$

Equation (2.2) is derived in Example 2.8.

Regulation requires at least as many controls as there are outputs. Since it is always possible to reduce the number of controls, we will henceforth assume $r = m$, so the system is square.

The following example illustrates the key ideas for robust regulation.

Example 2.5. *Regulation of SISO systems*

Consider a single input/single output system with reference signal generated by exogenous dynamics:

$$y_{ref} = \frac{1}{\phi(s)} = \frac{1}{(s+Z)}\vartheta_0$$

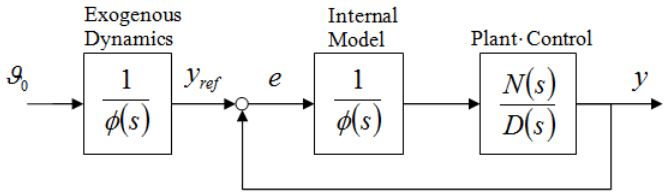

Figure 2.1: The Internal Model introduces zeros in the numerator of the closed loop transfer function to cancel poles of the exogenous dynamics.

where ϑ_0 is a constant. The exogenous dynamics Z are known but the initial conditions ϑ_0 may be unknown. The closed loop system is shown in Fig. 2.1.

The series connected control and plant are factored as $\frac{N(s)}{D(s)}$. The closed loop system in Fig. 2.1 has error dynamics

$$e = (y_{ref} - y) = \frac{D(s)\,\phi(s)}{D(s)\,\phi(s) + N(s)} \cdot \frac{1}{\phi(s)} \vartheta_0$$

where $\phi(s) = (sI_r - Z)$. Observe that the internal model introduces zeros to cancel the poles of the exogenous dynamics. Regulation requires cancellation of all roots of $\phi(s)$ in the closed right half plane C^+. The closed loop poles of $D(s)\,\phi(s) + N$ are stable by design. An example with reference and disturbance inputs is provided in [Che84] Chapter 9.6.

The following system definitions are needed for robust regulation of MIMO systems. These definitions are used throughout the remainder of this thesis.

Definition 2.6. *The compensator is a linear dynamic system that processes plant outputs and generates the control input u. The compensator states x_c are unique to the regulator design type*

- *explicit error model (η)*
- *observer of the plant and disturbance (x_o)*

as detailed in Sec. 2.2. Let

$$\bar{x} = \begin{bmatrix} x \\ x_c \end{bmatrix}$$

where the augmented state vector $\bar{x}$ is the plant state vector x plus either the augmented error states (η), or the observer states (x_o) which in the case of full state information may be just a disturbance estimate $\left(\hat{\vartheta}\right)$.

Definition 2.7. *Define the closed loop system consisting of plant, compensator, and exogenous system states Eqn. (1.2) as*

$$x_{cl} = \begin{bmatrix} \bar{x} \\ \vartheta \end{bmatrix} = \begin{bmatrix} x \\ x_c \\ \vartheta \end{bmatrix}$$

such that

$$\begin{aligned} \dot{x}_{cl} &= A_{cl} x_{cl} \\ e &= C_{cl} x_{cl} \end{aligned}$$

where

$$A_{cl} = \begin{bmatrix} \bar{A} & \mathcal{D} \\ 0 & Z \end{bmatrix}, \; C_{cl} = \begin{bmatrix} \bar{C} & F \end{bmatrix}$$

For example the error augmentation type regulator in Sec. 2.2.1, Eqn. (2.8) has

$$\mathcal{D} = \begin{bmatrix} E \\ JF \end{bmatrix}$$

The results of the preceding Example 2.5 are extended to MIMO systems in the following example. The sufficient condition derived here is the basis for the results of Sec. 2.3.

Example 2.8. *Sufficient Conditions for Regulation. This example follows Lemma 1 in [FW75a]. A necessary condition for regulation is*

$$\sigma^{+}\left(A_{cl}\right) \subset \ker C_{cl}$$

A state transformation is sought such that the above holds. Consider a translation which is a function of the exogenous inputs

$$z_1 = \bar{x} + \bar{X}\vartheta \tag{2.3}$$

where $\bar{x}$ is the compensator state vector and ϑ the exogenous system state vector. Write Eqn. (2.3) as a similarity transformation of the state

$$x_{cl} = Tz$$

where

$$T = \begin{bmatrix} I & -\bar{X} \\ 0 & I \end{bmatrix}, \qquad z = \begin{bmatrix} z_1 \\ z_2 \end{bmatrix}$$

such that

$$\begin{bmatrix} z_1 \\ z_2 \end{bmatrix} = T^{-1} \begin{bmatrix} \bar{x} \\ \vartheta \end{bmatrix} = \begin{bmatrix} I & \bar{X} \\ 0 & I \end{bmatrix} \begin{bmatrix} \bar{x} \\ \vartheta \end{bmatrix}$$

by blockwise inversion of T. Apply the transformation to A_{cl}

$$TA_{cl}T^{-1} = \begin{bmatrix} \bar{A} & -\bar{A}\bar{X} + \bar{X}Z + \mathcal{D} \\ 0 & Z \end{bmatrix}$$

Set the top right block to zero

$$\bar{A}\bar{X} - \bar{X}Z = -\mathcal{D}$$

and expand using the error augmentation type regulator (Sec. 2.2.1)

$$\begin{bmatrix} A+BK_x & BK_\eta \\ JC & Z \end{bmatrix} \begin{bmatrix} X \\ U \end{bmatrix} - \begin{bmatrix} X \\ U \end{bmatrix} Z = - \begin{bmatrix} E \\ JF \end{bmatrix} \tag{2.4}$$

Let

$$\bar{X} = \begin{bmatrix} X \\ U \end{bmatrix}$$

then set $Z = 0$ *for constant exogenous inputs and apply the factorization and simplification used in Eqn. (2.15) to rewrite Eqn. (2.4) as*

$$\begin{bmatrix} A & B \\ C & 0 \end{bmatrix} \begin{bmatrix} X \\ U \end{bmatrix} = - \begin{bmatrix} E \\ F \end{bmatrix}$$

which verifies Eqn. (2.2) of Thm. 2.4 and also is Eqn. (2.9). An alternate derivation is given in [Sal12], Section 3.2 which follows Lemma 1 of [Fra77].

2.2 Regulator Synthesis Types

Two types of regulator synthesis are identified in [KK78]:

- Error Augmentation, [Dav72]: The disturbance model Eqn. (1.2) is used explicitly as the controller. This controller is driven by the error dynamics, has r states, and an observer is not required.
- Disturbance Estimation, [Fra77]: The disturbance model Eqn. (1.2) is embedded in the observer. For a full order observer, the controller has $n + r$ states.

Note that the Error Augmentation synthesis permits variation in C in Eqn. (1.1) whereas the Disturbance Estimation synthesis does not.

The design of Error Augmentation type controllers for MMAR is completed below. The design of Disturbance Estimation type controllers is shown to be a Bilinear Matrix

Inequality in Section 4.4.2.

2.2.1 Error Augmentation

A robust regulator design procedure for a parameter dependent plant of type Eqn. (1.3) is given in [KK78], [Dav72] and has two steps:

1. Define an r dimensional, error driven dynamic system that incorporates the disturbance model,

$$\dot{\eta} = Z\eta + Je \tag{2.5}$$

   where J is chosen such that (J, Z) is controllable and e is defined in Eqn. (2.1).

2. Form the composite system from Eqn. (2.1)

$$\begin{bmatrix} \dot{x} \\ \dot{\eta} \end{bmatrix} = \begin{bmatrix} A_\theta & 0 \\ JC_\theta & Z \end{bmatrix} \begin{bmatrix} x \\ \eta \end{bmatrix} + \begin{bmatrix} B_\theta \\ 0 \end{bmatrix} u \tag{2.6}$$

   and solve for the stabilizing state feedback control...

$$u = \begin{bmatrix} K_x & K_\eta \end{bmatrix} \cdot \begin{bmatrix} x \\ \eta \end{bmatrix} \tag{2.7}$$

Example 2.9. *Show sufficiency of the error augmentation type regulator: Consider the closed loop system with plant Eqn. (1.1) with exogenous system Eqn. (1.2) and state feedback controller Eqn. (2.7),*

$$\begin{bmatrix} \dot{x} \\ \dot{\eta} \\ \dot{\vartheta} \end{bmatrix} = \left[\begin{array}{cc|c} A_\theta + B_\theta K_x & B_\theta K_\eta & E \\ JC_\theta & Z & JF \\ \hline 0 & 0 & Z \end{array}\right] \begin{bmatrix} x \\ \eta \\ \vartheta \end{bmatrix} \tag{2.8}$$

Let v_z be eigenvectors for the subspace $Z \subset A_{cl}$, i.e. $(A_{cl} - \lambda I)\, v = 0$ for $\lambda_z \in \sigma(Z)$ such

that $\lambda_z \notin \mathcal{C}^-$. By design (Z, J) is controllable, so J has full column rank and a right inverse $JJ^\dagger = I$. Observe that row two of the block matrix Eqn. (2.8) can be written

$$J \begin{bmatrix} C_\theta & J^\dagger (Z - \lambda_z) & F \end{bmatrix}$$

Hence all anti-stable eigenvalues λ_z have eigenvectors v_z in the nullspace of the output matrix,

$$v_z \subset \ker \begin{bmatrix} C_\theta & 0 & F \end{bmatrix}$$

which ensures $e = C_\theta x + F\vartheta$ goes to zero asymptotically.

2.2.2 Disturbance Estimation

A method of robust regulator synthesis for the system in Eqn. (2.1) given in [KK78], [Fra77] has three steps

1. Compute the steady state values for X, U from

$$\begin{bmatrix} A & B \\ C & 0 \end{bmatrix} \begin{bmatrix} X \\ U \end{bmatrix} + \begin{bmatrix} E \\ F \end{bmatrix} = 0 \tag{2.9}$$

2. Compute a state feedback gain K such that $A + BK_x$ is stable. The state feedback gain is then

$$u = U\vartheta + K_x (x - X\vartheta) \tag{2.10}$$

3. Compute an observer gain L to stabilize $A_o + LC_o$ where

$$A_o = \begin{bmatrix} A & E \\ 0 & Z \end{bmatrix}, \; B_o = \begin{bmatrix} B \\ 0 \end{bmatrix}, \; C_o = \begin{bmatrix} C & F \end{bmatrix}$$

$$x_o = \begin{bmatrix} \hat{x} & \hat{\vartheta} \end{bmatrix}^T, \; K = \begin{bmatrix} K_x & (U - K_x X) \end{bmatrix}$$

The spectrum of Z is now contained in the spectrum of the observer dynamics,

$$\sigma(Z) \subset \sigma(A_o + LC_o + B_oK)$$

The null space of C_o must be known a priori for proper placement of the disturbance model Z eigenvectors for this synthesis method.

2.3 Loss of Simultaneous Regulation

Previous research on regulator theory has clarified the importance of zero structure for regulator design. The effect of zero structure on set-point regulation is explored in Chapter 7.2 of [KS72]. The relationship between regulator structure and zero structure is resolved for linear systems with linear exogenous inputs in [Fra77]. Further clarification of the regulator and zero structure relationship is provided in [FW75b]. Necessary zero structure conditions for local regulation of nonlinear systems with linear compensators is detailed in [KBB91]. Furthermore [KBB91] provides a realistic example of zero structure change and the loss of simultaneous regulation.

The results presented in this section originate in the requirements for robust regulation of Theorem 2.4 derived in Example 2.8. Theorem 2.4 specifies the open loop system $\{A, B, C\}$ for which robust regulation is possible. Now consider robust regulation failure. Two definitions are needed.

Following [Ber93] define a parameter dependent linear matrix pencil.

Definition 2.10. *The system matrix for $\{A_\theta, B_\theta, C_\theta\}$ can be written in the form of a matrix pencil as*

$$\Gamma_\theta(s) = \begin{bmatrix} sI - A_\theta & B_\theta \\ C_\theta & 0 \end{bmatrix} \tag{2.11}$$

The more common form of a system matrix is just the constant term in Eqn. (2.11), i.e. $\Gamma_\theta(0)$. Since this thesis considers only constant disturbances, we are generally interested in

$\Gamma_\theta(s)$ *at* $s = 0$. *Thus, system matrix* $\Gamma_\theta(0)$ *and parameter dependent pencil* $\Gamma_\theta(s)$ *are used interchangeably in this report.*

Regulation requires that Eqn. (2.2) be solvable for any E, F, and θ. This requirement can also be written as

$$\begin{bmatrix} E \\ F \end{bmatrix} \in Im \begin{bmatrix} sI - A_\theta & B_\theta \\ C_\theta & 0 \end{bmatrix} \tag{2.12}$$

for all s and possible values of θ. Of course the values of s for which $\Gamma_\theta(s)$ loses rank are the transmission zeros. The set of θ for which regulation fails may now be defined.

Definition 2.11. *The set of points in parameter space on which regulation fails is the* singular surface*,*

$$\left\{\theta \in R^k : \det \Gamma_\theta(0) = 0\right\} \tag{2.13}$$

The system matrix $\Gamma_\theta(0)$ can lose rank due to a zero at the origin and also due to a defect in the input B_θ or output C_θ matrices. Observe that if B_θ is column rank deficient or C_θ is row rank deficient, then $\Gamma_\theta(s)$ loses rank for all values of s. Since Γ_θ is either a regular or singular pencil for fixed θ, the singular surface partitions the parameter space into disjoint sets.

Observe that the dimension of Eqn. (2.11) is $n+p$ equations. And this set of $n+p$ linear equations has $n+p+k$ variables. Thus the equilibrium surface is dimension k. Furthermore, the singular surface adds the additional (nonlinear) constraint Eqn. (2.13) such that the singular surface is dimension $k-1$ since

$$(n+p+k) - (n+p+1) = k - 1$$

or codimension one in the parameter space. For a rigorous statement of the above see [BK94].

Theorem 2.12 parallels [BK94].

Theorem 2.12. *Consider a region of the parameter space bisected by the singular surface. A robust regulator designed for one half of the space will be unstable in the adjacent half space for generic systems.*

The singular surface divides the original family of plants into sub-families. A robust regulator designed for Eqn. (2.1) and applied to Eqn. (1.3) will fail to stabilize adjacent sub-families.

Proof: Loss of simultaneous regulation at a singular surface is introduced in [KBB91] and proved in [BK94]. Example 2.14 above is a sufficient proof for the Error Augmentation type regulator.

Example 2.13. *Singular Surfaces as Partitions*

A single linear controller is unable to simultaneously regulate plants on either side of the singular surface. The controller designed for plant p_a fails to stabilize plant p_b as shown in Fig. 2.2.

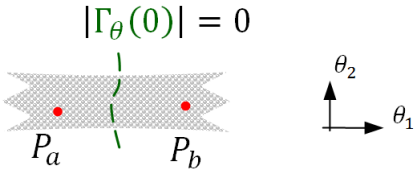

Figure 2.2: Singular Surfaces Partition the Parameter Space

Singular surfaces partition the family of plants $\mathcal{P}$ into equivalence classes. Traversing a singular surface is a sufficient but not a necessary condition for loss of stability. Loss of stability is certain at the singular surface. Loss of stability is possible within an open region of the parameter space. In summary, the singular surface partitions the parameter space. The resulting disjoint regions are a starting point for multiple model controller selection.

Example 2.14. *Loss of Simultaneous Regulation in Error Augmentation Type Regulator*

According to Theorem (2.12), traversal of the singular surface is sufficient for loss of stability. The plant and compensator closed loop system $\dot{x}_{cl} = A_{cl}x_{cl}$ *with state* $x_{cl} = \begin{bmatrix} x & \eta \end{bmatrix}^T$ *has dynamics matrix* A_{cl}*:*

$$\begin{bmatrix} A_\theta + B_\theta K_x & B_\theta K_\eta \\ JC_\theta & Z \end{bmatrix} \tag{2.14}$$

Recall that $Z = 0_r$ *for step reference signals and constant disturbances. Factor Eqn. (2.14) as*

$$\begin{bmatrix} I & 0 \\ 0 & J \end{bmatrix} \cdot \begin{bmatrix} A_\theta & B_\theta \\ C_\theta & 0 \end{bmatrix} \cdot \begin{bmatrix} I & 0 \\ K_x & K_\eta \end{bmatrix} \tag{2.15}$$

where J *is dimension* $r \times p$*,* K_η *is dimension* $p \times r$*, and both* J*,* K_η *are full rank by design. Generically the singular surface is intersected transversely and one parameter at a time. Thus Eqn. (2.15) losses rank when* $\det \Gamma_\theta(0) = 0$ *by application of rank inequalities.*

The regulator design of Sec. 4 will be robust to perturbations in all elements of the matrices $\{A_\theta, B_\theta, C_\theta\}$ including variation in the k parameters θ if an internal model design per Thm. 2.3 is used on a plant subject to the conditions of Thm. 2.4.

3. MULTIPLE MODEL ADAPTIVE CONTROL

Multiple Model Adaptive Control (MMAC) is surveyed in Sec. 1.3. This chapter details our implementation of MMAC with LQR control design and Lyapunov switching logic.

3.1 Covering

Due to a loss of simultaneous regulation described by Theorem 2.12, a multiple model approach is employed to regulate the family of plants $\mathcal{P}$. The methods summarized in Sec. 1.3.2 design controllers for a finite set of plant models and then employ robustness metrics to ensure $\mathcal{P}$ is covered. The controllers proposed in this thesis are designed for a finite set of convex polytopes Ω_i in the parameter space as defined in Sec. 4.2 such that $\mathcal{P} \subseteq \{\mathbf{p}(\theta) \,|\theta \in \bigcup \Omega_i\}$. This covering method facilitates accommodation of singular surfaces in the parameter space. Figure 3.1 contrasts the parameter space covering method outlined in 1.3.2 with the convex approach used here.

Advantages of convex regions Ω_i include flexibility in shaping, less overlap than operator norms (e.g. $\|\cdot\|_2$), and efficient computation due to underlying convexity.

A disadvantage of this covering method is that a Common Quadratic Lyapunov Function (CQLF) must exist for all $\mathbf{p}(\theta) \in \Omega_i$. This CQLF requirement is stronger than exponential stability and may increase the cardinality of $\mathcal{C}$.

Designing controllers to cover the parameter space is simplified by the use of convex polytopes. But how can these linear shapes be accommodated in a solution to the quadratic LQR problem? The following two claims form the basis for the convex covering method detailed in Chapter 4.

Claim 3.1. *The map from parameters to the set of plants $\theta \to \mathbf{p}(\theta)$ is linear in θ. For*

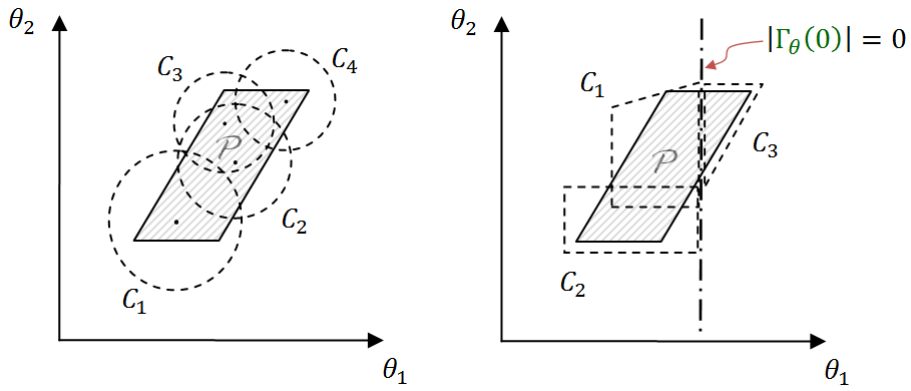

Figure 3.1: Parameter Space Covers: (Left) Robustness metrics [Sec. 1.3.2]; (Right) Improved Convex method

example, a basis can be found for each parameter dependent matrix such that

$$A(\theta) = A_0 + \sum_{1}^{k} \theta_i A_i \tag{3.1}$$

where A_0 is the nominal system and for $i = \{1 \dots k\}$ the θ_i are components of parameter vector θ. Technically the above form is affine but can always be expressed as linear by the augmented parameter vector $(\bar{\theta})^T = [1\ \theta]$ with $1 \cdot A_0$. Verify that $A(\theta)$ is linear in θ

$$\begin{aligned} A(\theta' + \theta'') &= A(\theta') + A(\theta'') \\ A(c\theta) &= cA(\theta) \end{aligned}$$

and thus $A(\theta)$ etc., $\Gamma(\theta)$, and $\mathbf{p}(\theta)$ are linear by Eqns. (1.1) and (2.11). Linearity of the family of plants in the parameter θ implies convexity in θ which is important for Sec. 4.3.

Claim 3.2. *Linear Matrix Inequalities, which are linear in parameters, encode quadratic*

equations. Consider the Schur complement of a partitioned matrix M by factoring

$$M = \begin{bmatrix} M_{11} & M_{12} \\ M_{21} & M_{22} \end{bmatrix} = \begin{bmatrix} I & M_{12}M_{22}^{-1} \\ 0 & I \end{bmatrix} \begin{bmatrix} M_{11} - M_{12}M_{22}^{-1}M_{21} & 0 \\ 0 & M_{22} \end{bmatrix} \begin{bmatrix} I & 0 \\ M_{22}^{-1}M_{21} & I \end{bmatrix}$$

where M_{22} is nonsingular. The determinant of M is now straightforward. When M is symmetric, for example $M_{12} = M_{21}^T$, the determinant of M contains quadratic terms.

A linear matrix inequality (LMI) is a set of inequalities written in matrix form

$$L(m) = L_0 + \sum_{1}^{i} m_i L_i > 0 \tag{3.2}$$

where each L_i, $i = \{0, \ldots l\}$ are symmetric matrices. Variables L, m, and i are specific to inequality Eqn. (3.2). Matrix L is positive definite if $x^T M(x)\, x > 0$ for all $x \neq 0$. The set of scalars m_i of dim i that satisfy inequality Eqn. (3.2) are convex. That is the $\{m | L(m) > 0\}$ is a convex set.

Example 3.3. *Linear Matrix Inequality and the Stability of Convex Combinations of Matrices. Consider the stability condition*

$$A_\theta^T P + P A_\theta < 0 \tag{3.3}$$

Observe that a basis for a 2×2, symmetric $P > 0$ is

$$P = p_{11} \begin{bmatrix} 1 & 0 \\ 0 & 0 \end{bmatrix} + p_{12} \begin{bmatrix} 0 & 1 \\ 1 & 0 \end{bmatrix} + p_{22} \begin{bmatrix} 0 & 0 \\ 0 & 1 \end{bmatrix}$$

As an example of the linearity of Claim 3.1, let

$$A_\theta = \theta A_0 + (1 - \theta) A_1 \tag{3.4}$$

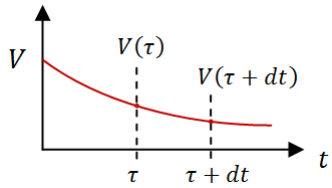

Figure 3.2: Stable Lyapunov Function

then if inequality Eqn. (3.3) holds for each $\theta \in \{0,1\}$ *and a common* P *it will hold for all* $\theta \in [0,1]$. *Since inequality Eqn. (3.3), which is linear in* θ *per Eqn. (3.2), holds for each dynamic system* $\dot{x} = A_\theta x$ *where* $A_\theta = \{A_0, A_1\}$, *it holds for all systems where* $A_\theta \in Co\{A_0, A_1\}$. *Note that the more general question of stability of linear combinations of matrices not subject to a common quadratic Lyapunov function is an open research problem, for example [BFS88].*

An example of encoding of quadratic functions in an LMI per Claim 3.2 is given in Sec. 4.1.

3.2 Switching

3.2.1 Switch Logic

A CQLF produces a scalar metric that can be tested to ensure stability. A Lyapunov function for the i'th convex polytope Ω_i with final state x_f

$$V_i = (x - x_f)^T P_i (x - x_f) \tag{3.5}$$

is monitored for the "in the loop" controller. Each controller is paired with a Lyapunov function. If the Lyapunov function is decrescent, i.e. $V_i(\tau + dt) < V_i(\tau)$ as shown in Fig. 3.2, then the correct controller has been identified.

If the "on" Lyapunov function ceases to be decrescent, a different controller is switched on. At least one stabilizing controller exists by design. The controllers must be tried "in

the loop." For linear systems with no measurement noise a sophisticated switch logic is unnecessary. A stabilizing controller will eventually be implemented.

Bounds on the time rate of change of the quadratic Lyapunov function may be computed [Kha02], [SL91]. For a Lyapunov function with

$$0 \leq V(x) \leq k_2 \|x\|_2 \text{ , and } \tfrac{d}{dt} V(x) \leq -k_3 \|x\|_2 \text{ ,}$$

$$\dot{V} \leq -\frac{k_3}{k_2} V \tag{3.6}$$

Here $k_2 = \lambda_{max} P$ and $k_3 = \lambda_{min} Q_z$ where P and Q_z are symmetric positive definite matrices. The design weight Q_z equals $C_z^T C_z$ of Sec. 4.1. The test for a stabilizing controller is

$$x(\tau + dt)^T P x(\tau + dt) \leq \gamma x(\tau)^T P x(\tau) \tag{3.7}$$

where

$$e^{-\frac{\lambda_{min} Q_z}{\lambda_{max} P} \cdot dt} < \gamma < 1 \tag{3.8}$$

Note that this switching strategy guarantees Lyapunov stability with convergence rate no less than γ. A stabilizing controller will be implemented, but this controller may not be the "true" or "optimal" controller.

An implementation challenge of Eqn. (3.5) is the a priori requirement of knowledge of x_f. This challenge is discussed in Sec. 3.2.2 below.

3.2.2 Estimate Final State

A key benefit of robust regulation is that a priori knowledge of the final state x_f is not necessary. However, the Lyapunov switch logic function Eqn. (3.5) requires knowledge of x_f. The final state $x_f = \lim_{t \to \infty} x(t)$ is a function of unknown parameters, controller gains, and the exogenous input. The main results of this thesis, the regulator design of Chapter 4, is independent of knowledge of ϑ. Example problems in Chapters 6 & 7 assume that the

unknown component of ϑ is small in relation to Eqn. (3.6).

The Observer Dynamics synthesis method (Sec. 2.2) provides an estimate of the exogenous input ϑ but is a Bilinear Matrix Inequality (BLMI) as shown in Sec. 4.4.2 and will not be considered here. Two methods to estimate the final state are provided below:

1. State transformation to a form suitable for removing the effect of translations in the equilibrium state x_f
2. Exploit the convexity of V in x_f

State Transformation

Geometry The closed loop Error Augmentation regulator outlined in Sec. 2.2.1 can be written as follows

$$\dot{x}_{cl} = A_{cl} x_{cl}$$

where $x_{cl} = [x\ \eta\ \vartheta]^T$ and

$$\left[\begin{array}{c} \dot{x} \\ \dot{\eta} \\ \dot{\vartheta} \end{array}\right] = \left[\begin{array}{cc|c} A + BK_x & BK_\eta & E \\ JC & Z & -JF \\ \hline 0 & 0 & Z \end{array}\right] \left[\begin{array}{c} x \\ \eta \\ \vartheta \end{array}\right] \tag{3.9}$$

where η are the internal model states and ϑ is the disturbance state. The state vector has dimension $n + (r \cdot p) + r$ where r is the dimension of the disturbance. The following analysis also holds for the disturbance estimation type regulator.

The closed loop system Eqn. (3.9) is designed such that

1. Eigenvectors with eigenvalues $\lambda = 0$ are placed in the $\ker C$. The equilibrium state x_f translation is contained in the space of these eigenvectors denoted as v_0 and referred to as rigid modes.
2. The remaining eigenvectors have eigenvalues $\lambda \in \mathbb{C}^-$ and are denoted v_i and referred to as stable modes.

We are interested in the behavior of Eqn. (3.9) under parametric perturbation of plant matrices $\{A, B, C\}$ and disturbance mapping matrices $\{E, F\}$. Previous work obtains a CQLF for systems with parametric perturbation in $\{A, B, C\}$, but requires a priori knowledge of the final state (x_f). Translations in the final state are due to changes in $\{E, F\}$.

Two issues exist in isolating the rigid modes from the stable modes:

- The eigenvectors v_0 with eigenvalues $\lambda = 0$ may change when $\{E, F\}$ are perturbed. Consider a decomposition of the state space

$$\mathcal{X}_{cl} = \Theta_0 \oplus \Theta_0^{\perp}$$

  Here $v_0 \in \Theta_0$ contains the rigid modes and the orthogonal complement $\Theta_0^{\perp}$ contains the stable modes. Formally, the subspace $\Theta_0^{\perp} = \text{Span}\{v_i\}$ where eigenvectors v_i have eigenvalues $\lambda_i \in \mathbb{C}^-$. Thus $\Theta_0^{\perp}$ is a convenient subspace for a Lyapunov function since $x_f = 0$. However, since perturbation in $\{E, F\}$ change Θ_0 and hence $\Theta_0^{\perp}$, this decomposition is infeasible since a constant, precisely known disturbance map $\{E, F\}$ is not a reasonable design requirement.

- While by definition the set of eigenvectors $\{v_i\}$, $i = \{0, \ldots, n + r \cdot p\}$ of A_{cl} are invariant under A_{cl}, the eigenvectors are not orthogonal. Thus, changes to v_0 due to perturbation in $\{E, F\}$ are projected onto the v_i.

Transformation While a parameter invariant division between rigid and stable modes is not possible, perhaps the system can be transformed into a more useful representation. The following outlines a transformation that may be suitable for a yet to be determined estimation or output injection (adaptive perhaps) method to compensate for the rigid modes. The transformation is developed for an error augmentation regulator but also holds for a disturbance estimation regulator.

- Given

$$A_{cl} = \left[\begin{array}{cc|c} A + BK_x & BK_\eta & E \\ JC & Z & -JF \\ \hline 0 & 0 & Z \end{array}\right]$$

- Compute the eigenvectors (v) and eigenvalues (λ) of A_{cl} where$(A_{cl} - \lambda I)\, v = 0$. Assemble the eigenvectors columnwise to compute the transformation

$$T^{-1} = \left[\begin{array}{ccc} v_i & \cdots & v_0 \end{array}\right]$$

- Obtain A_{cl} in the modal coordinates $z = Tx_{cl}$ such that $A_z = TA_{cl}T^{-1}$ where A_z is a diagonal matrix of eigenvalues

$$A_z = \left[\begin{array}{cc} \Lambda_{\mathbb{C}^-} & 0 \\ 0 & \lambda_0 \end{array}\right]$$

where $\Lambda_{\mathbb{C}^-}$ is a diagonal matrix for the Hurwitz eigenvalues, $\lambda_i \in \mathbb{C}^-$, $i \in \{1, \ldots, n-1\}$,

$$\Lambda_{\mathbb{C}^-} = \left[\begin{array}{ccc} \lambda_1 & & 0 \\ & \ddots & \\ 0 & & \lambda_{n-1} \end{array}\right]$$

and matrix λ_0 collects the internal model eigenvalues in an $(r+p) \times (r+p)$ matrix of zeros.

Now consider the effects of perturbations of plant matrices $\{A, B, C\}$ and disturbance mapping $\{E, F\}$ on the transformed system. Apply the transformation T computed above to obtain

$$A_z = \left[\begin{array}{cc} \Delta_{\mathbb{C}^-} & a\,(\star) \\ 0 & \lambda_0 \end{array}\right] \tag{3.10}$$

where $\Delta_{\mathbb{C}^-}$ is no longer a diagonal matrix. The off diagonal block $a(\star)$ with $\dim a(\star) = (n + p \cdot r) \times (p \cdot r)$ is a function of perturbations in $\{A, B, C\}$ and $\{E, F\}$. In the case $\{A, B, C\}$ and $\{E, F\}$ are known, $a(\star) = 0$ and the transformed states z with $\lambda_i \in \mathbb{C}^-$ have final value zero. In the case $\{A, B, C\}$ and $\{E, F\}$ have known bounds, the transformed states z with $\lambda_i \in \mathbb{C}^-$ have final value within a known bound of the origin.

The eigenvalues of $\Delta_{\mathbb{C}^-}$ are the perturbed eigenvalues of A_z. The covering Sec. 3.1 obtains a CQLF for the stable subspace of A_{cl} in a region Ω_i. The similarity transformation of the state T can also transform the CQLF matrix P to apply to the transformed $\Delta_{\mathbb{C}^-}$.

For a system matrix with form

$$\Gamma = \left[\begin{array}{c|c} A_z & B_z \\ \hline C_z & 0 \end{array}\right]$$

the transformed, perturbed system can be written

$$\Gamma = \left[\begin{array}{cc|c} \Delta_{\mathbb{C}^-} & a(\star) & b(T) \\ 0 & \lambda_0 & 0 \\ \hline c(T) & 0 & 0 \end{array}\right] \tag{3.11}$$

where $a(\star)$ is defined above. The $b(T)$ and $c(T)$ are $(n + p \cdot r) \times m$ and $n \times (n + p \cdot r)$ matrices respectively. The $b(T)$ and $c(T)$ vary with plant parameters in $\{A, B, C\}$ and are independent of changes in $\{E, F\}$. Elements of $b(T)$ and $c(T)$ are different than elements of B_z, C_z in general due to the similarity transformation T.

Note that the transformed output

$$\left[\begin{array}{cc} c(T) & 0 \end{array}\right] = TC_z$$

lies in the subspace with stable modes $\Theta_0^{\perp}$. The rigid modes do not appear in the transformed output due to the eigenvector placement discussed in the introduction. The trans-

formed output contains only stable modes such that regulation $\lim_{t\to\infty} y \to 0$ where $y = TC_z$ is preserved.

The transformed input is also a function of T and the (un)controllability of rigid modes are unchanged by similarity transformation.

Application The application of transformed system Eqn. (3.11) to remove the effects of the translation of the equilibrium state x_f on the switch logic are explored in this chapter. Assume full state knowledge. Suggestions for future research are provided.

Consider systems of the form discussed in [KB00], pg. 248,

$$\dot{z} = \bar{A}z + E\Psi\left(\vartheta - \hat{\vartheta}\right) \tag{3.12}$$

where $\sigma\left(\bar{A}\right) \in \mathbb{C}^-$ and choose the parameter update law

$$\dot{\hat{\vartheta}} = Q\Psi^T\left(\xi, z, \hat{\vartheta}, u\right) E^T P z \tag{3.13}$$

which ensures the Lyapunov stability of

$$V = z^T P z + \left(\vartheta - \hat{\vartheta}\right) Q^{-1} \left(\vartheta - \hat{\vartheta}\right) \tag{3.14}$$

Observe the similarity between Eqn. (3.10) and

$$\dot{z} = \left(\Delta_{\mathbb{C}^-}\right) z + a\left(\star\right)\vartheta$$

which can be written with parameter estimate $\hat{\vartheta}$ as

$$\dot{z} = \left(\Delta_{\mathbb{C}^-}\right) z + a\left(\star\right)\left(\vartheta - \hat{\vartheta}\right)$$

Unfortunately the Lyapunov function Eqn. (3.14) contains the unknown ϑ and cannot be used as a switch metric. A variable structure observer may help to test the convergence of

z.

Note that in the linear case the parameter update Eqn. (3.13) is a passive function as defined in [Kha02], pg. 236.

Lyapunov Function Convexity

A method to estimate x_f directly based on the convexity of V in Eqn. (3.5) in x_f is outlined below.

Proposition 3.4. *Given a Lyapunov function*

$$V(t) = (x(t) - x_f) P (x(t) - x_f) \tag{3.15}$$

then $V(t)$ is a convex function in x_f for fixed $x(t)$ and P.

Proof. For ease of computation, let the symmetric, positive definite P be a diagonal matrix. (Symmetric matrices are diagonalizable by state transformation.) The second derivative test of $V(t)$ with respect to x_f is $2P$; hence $V(t)$ is (strictly) convex in x_f. A convex solver can quickly ascertain if an x_f exists such that $V(t)$ is decrescent. □

The x_f are constrained to lie in the $\bar{A}$ invariant $\ker C$. Additional algebraic constraints, i.e. aircraft pitch rate $q = 0$ at equilibrium, may improve the estimate of x_f.

As previously noted, a sequence of measured states $x(\tau)$, $x(\tau + dt)$, $x(\tau + 2dt)$, etc form the set of equations

$$\gamma V(\tau) > V(\tau + dt), \gamma V(\tau + dt) > V(\tau + 2dt), \ldots \tag{3.16}$$

This set of equations is a convex minimization problem for x_f. The above inequalities contain quadratic terms in x_f.

If $\gamma = 1$, the quadratic terms x_f^2 of inequalities (3.16) cancel and only linear terms of x_f remain. The set of inequalities (3.16) with $\gamma = 1$ may be written

$$V(\tau) > V(\tau + dt) > V(\tau + 2dt) \ldots \tag{3.17}$$

and quickly solved for x_f. The computational advantages of Eqn. (3.17) must be weighed against the tighter bounds of Eqn. (3.16).

Furthermore, meaningful physical bounds on the elements of the disturbance maps $\{E, F\}$ can be used to bound the convex estimation problem.

Algebraic constraints on x_f such as output error $e(x(t), x_f) = 0$ as $t \to \infty$ may also be enforced when solving inequalities Eqns. (3.16) or (3.17).

Remark 3.5. *The set of inequalities (3.16) is insufficient to guarantee convergence for closed-loop unstable systems. Consider a scalar system with state divergence along the real axis. Inequalities Eqns. (3.16) and (3.17) are relative and not absolute. All that is required is the distance $x(t) - x_f$ shrink at successive intervals. In this manner x_f could always be chosen just beyond the extremum x of the sequence $x(t)$. In the case of n states, the addition of $p < n$ output error constraints $e = y - y_{ref}$ is insufficient to prevent divergence.*

One method to prevent divergence of the estimate of x_f is to enforce convergence of successive Lyapunov function differences. For a strictly decreasing Lyapunov function V, $\dot{V} < 0$, successive differences must shrink as time grows,

$$V(\tau + dt) - V(\tau + 2dt) < V(\tau) - V(\tau + dt) \tag{3.18}$$

In summary, inequalities (3.16) and (3.18) are sufficient to ensure a successful Lyapunov switch logic. Enforcing known algebraic identities such as output or state constraints may significantly improve switch logic accuracy. Preliminary studies suggest that the length of time required to reject controllers unable to regulate the plant is undesirable. A geometric study may provide further insights.

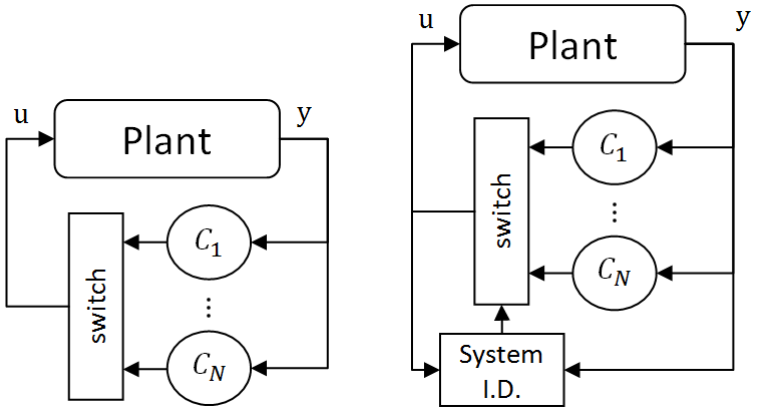

Figure 3.3: Baseline (left) and System Identification (right) forms of MMAC

3.2.3 Switch Logic Augmentation

If the number of plant models and subsequent controllers is small, a trial and error Lyapunov level set switch logic is adequate. However a larger controller set may require a more sophisticated switch logic. Our MMAC framework is helpful for adding a system identification algorithm to improve switch logic accuracy. Figure 3.3 shows the MMAC baseline on the left and MMAC with system identification on the right:

Identification algorithms assume stable systems to ensure signal boundedness. In the MMAC framework, an unstable plant/controller combination has a bounded signal due to the Lyapunov level set switch logic. Hence, the designer is free to choose a system identification algorithm to inform the switch logic.

The system identification problem for multiple model adaptive regulation may be unique in several ways:

- A subfamily of plants has known relative order and zero structure.
- The number of parametric unknown plant parameters may be smaller than plant coefficients (a_{11}, etc.) and may even be less than the number of states. Robust

regulation compensates for perturbations to coefficients other than the parametric unknowns.

- Switching between controllers generates a discontinuous form of Persistent Excitation.
- Model inaccuracy is given in the time domain (state space) instead of classical frequency domain and $\mathcal{H}_\infty$ techniques.

These unique features, in particular the lower dimensional set of unknown parameters, may facilitate model identification.

Three distinct lines of research were considered from the significant literature on system identification.

1. Subspace Identification, which uses the Hankel matrix to solve for the observability and then controllability matrices. Matlab code is available with the book [VODM96].
2. "Model Invalidation," A Nevanlinna-Pick-Caratheodory interpolation result on systems with additive perturbations [PKT$^+$94].
3. Linear Parameter Varying (LPV) system identification, such as the application of gradient methods in [BG02]

The sources listed above and their references and citations can be explored for more information. Subspace Identification was tested with 5-10% error despite lack of persistent excitation. This may be sufficient to improve the final state estimation algorithm of Sec. 3.2.2.

4. REGULATOR DESIGN

A Common Quadratic Lyapunov Function (CQLF) is sought for subfamilies of the parameter dependent family of plants Eqn. (1.1). The next three sections adapt the LMI method in [BEFB94], pg. 115 to provide state feedback gains and CQLFs for systems described by Eqn. (1.3). The final section gives an in-depth example.

4.1 LQR as LMI

The quadratic LQR problem can be expressed as a Linear Matrix Inequality (LMI). Given a linear system

$$\dot{x} = Ax + Bu,\ z = C_z x + D_z u \tag{4.1}$$

with state feedback control $u = Kx$ the LQR problem of minimizing the energy

$$\int_0^\infty z^T z\, dt$$

can be solved by the inequality

$$\begin{bmatrix} A\Phi + \Phi A^T + BY + Y^T B^T & (C_z\Phi + D_z Y)^T \\ C_z\Phi + D_z Y & -I \end{bmatrix} < 0 \tag{4.2}$$

which is a function of system parameters A & B, design weights C_z & D_z, and is convex in the symmetric matrix variable $\Phi > 0$. Here $Y = -\left(D_z^T D_z\right)^{-1} B^T$ with Lyapunov matrix $P = \Phi^{-1}$. The design weights C_z, D_z chosen such that

$$D_z^T C_z = 0 \tag{4.3}$$

as in Eqn. (6.1).

Proposition 4.1. *[BEFB94] The LMI (4.2) is equivalent to the quadratic Riccati matrix*

inequality via the Schur complement

$$A^T P + PA + C_z^T C_z - PB\left(D_z^T D_z\right)^{-1} B^T P \leq 0 \tag{4.4}$$

The LQR state feedback controller is $K = Y\Phi^{-1} = -\left(D_z^T D_z\right)^{-1} B^T P$.

Proof. The block matrix

$$\begin{bmatrix} A_{11} & A_{12} \\ A_{21} & A_{22} \end{bmatrix}$$

is negative definite according to the Schur complement if

$$\begin{aligned} A_{22} &< 0 \\ A_{11} - A_{12}A_{22}^{-1}A_{21} &< 0 \end{aligned}$$

Verify the second inequality where

$$\begin{aligned} A_{11} &= A\Phi + \Phi A^T + BY + Y^T B^T \\ A_{12} &= (C_z\Phi + D_z Y)^T \\ A_{21} &= (C_z\Phi + D_z Y) \\ A_{22} &= -I \end{aligned}$$

Expand the product

$$\begin{aligned} -A_{12}A_{22}^{-1}A_{21} &= -(C_z\Phi + D_z Y)^T(-I)(C_z\Phi + D_z Y) \\ &= \Phi^T C_z^T C_z \Phi + \Phi^T C_z^T D_z Y + Y^T D_z^T C_z \Phi + Y^T D_z^T D_z Y \end{aligned}$$

Observe that

- the term $\Phi^T C_z^T C_z \Phi$ is the third term in Eqn. (4.4)

- the terms $\Phi^T C_z^T D_z Y$ and $Y^T D_z^T C_z \Phi$ are zero due to Eqn. (4.3)
- the terms $Y^T D_z^T D_z Y$ and $BY + Y^T B^T$ add to become $-PB\left(D_z^T D_z\right)^{-1} B^T P$

where $Y = -\left(D_z^T D_z\right)^{-1} B^T$ as before, $Y^T = -B\left(D_z^T D_z\right)^{-1}$, and the identities $(XY)^{-1} = Y^{-1}X^{-1}$ & $(XY)^T = Y^T X^T$ have been used.

□

4.2 Block LMI

The LQR design problem is cast as an LMI in Eqn. (4.2) for a single plant. In this section the LQR design problem is cast as an LMI for a set of plants. A double index notation will be used for parameter space coordinates θ_{ij} where the index j signifies the vertex and the index i signifies the region Ω_i. Composition of regions Ω_i are explored in more detail in the following Sec. 4.3. This section extends inequality Eqn. (4.2) to a subfamily of plants.

Definition 4.2. *The image of the set of vertices* $\{\theta_{ij}\}$ *under* $\mathbf{p}(\cdot)$ *is the set of plants* $\{\mathbf{p}(\theta_{ij})\}$. *A set of LMIs for* $\{\mathbf{p}(\theta_{ij})\}$ *is a* block LMI.

In particular, consider the block LMI where the inequality Eqn. 4.2 is enforced at each vertex θ_{ij} *in* Ω_i,

$$\begin{bmatrix} LMI(\theta_{i1}) & & \\ & LMI(\theta_{i2}) & \\ & & \ddots \end{bmatrix} < 0 \tag{4.5}$$

This block LMI is formed by substituting

$$A \to \bar{A}(\theta_{ij}), \quad B \to \bar{B}(\theta_{ij})$$

into Eqn. (4.2) at vertices $\theta_{ij} \in \{\theta_{i1}, \theta_{i2}, \ldots, \theta_{iv_i}\}$ to obtain a set of inequalities for simultaneous solution. Details of $\bar{A}(\theta_{ij})$, $\bar{B}(\theta_{ij})$ are left to Sec. 4.4.1.

Each block LMI Eqn. (4.5) solves for a stabilizing controller $C_i \in \mathcal{C}$ with state feedback control K_i and Lyapunov function matrix P_i for the continuous set of plants $\{\mathbf{p}(\theta) | \theta \in \Omega_i\}$. The state feedback control is

$$K_i = -\left(D_z^T D_z\right)^{-1} B_i^T P_i \tag{4.6}$$

and the Lyapunov function matrix is $P_i = Q_i^{-1}$. Choose a B_i such that

$$B_i \in Co\{B(\theta_{ij})\} \tag{4.7}$$

to obtain a constant K_i. It can be shown (Sec. 4.3.1 below) that if Eqn. (4.5) holds for all $B(\theta_{ij})$ and B_i is chosen according to Eqn. (4.7), then a solution P_i of the block LMI

$$A_{CL}^T(\theta_{ij}) P_i + P_i A_{CL}(\theta_{ij}) + C_z^T C_z < 0 \tag{4.8}$$

with

$$A_{CL}(\theta_{ij}) = A(\theta_{ij}) + B(\theta_{ij}) K_i \tag{4.9}$$

exists. The P_i of Eqn. (4.8) may need to be used in place of the P_i of Eqn. (4.5) for the switch logic of Sec. 3.2 if either $\{B(\theta_{ij})\}$ is nonsingleton or if the $LMI(\theta_{ij})$ in Eqn. (4.5) are assigned different C_z, D_z, i.e. $D_z(\theta_{ij})$.

The distinction between LMI and block LMI is convenient for assembling the inequalities. A numerical solver makes no distinction between an LMI and a set of LMIs.

4.3 Finite Set of Plants

The previous Sec. 4.2 obtains an CQLF for a finite set of plants, but the coordinate set $\{\theta_{ij}\}$ used to define region Ω_i is not defined. Obtaining $\{\theta_{ij}\}$ to represent region Ω_i is the goal of this section. Only linear plants (Eqn. (1.1)) are considered here. Nonlinear plants (Eqn. (1.4)) are considered in Chapter 7.

As shown in Sec. 3.1, Claim 3.1, a linear map from the parameter space to the set of parameter dependent plants is assumed known. And linearity is preserved in the LMI. Hence the map from parameter space to the controller design Eqn. (4.5) is linear and thus convex. Since the LMI is convex, design equation Eqn. (4.5) needs to be verified only at the vertices of a convex region in the parameter space. The polytopic region Ω_i is defined by the convex hull (Co) of its vertices, i.e.

$$\Omega_i \equiv Co\left\{\theta_{ij}\right\} \tag{4.10}$$

Thus a small set of polytope vertices $\{\theta_{ij}\}$ used in the block LMI computation Eqn. (4.5) may "cover" an arbitrarily large subspace of the parameter space.

Since robust regulation is used the variation in $\{E, F\}$ does not need to be constrained. Figure 3.1 is an example of convex regions Ω_i described by Eqn. (4.10).

When $\mathcal{P}$ has a diverse zero structure two or more regions Ω_i will be needed. Per Theorem (2.12), if for any $\theta \in \Omega_i$, $|\Gamma_\theta(0)| = 0$, then Ω_i contains singular surface and neither a common regulator nor a CQLF exist for all $\theta \in \Omega_i$. The singular surface is a natural partition for plant subfamilies.

4.3.1 Choice of B_i

A specific B must be chosen for the constant LQR state feedback control $K = -\left(D_z^T D_z\right)^{-1} B^T P$ that stabilizes the set of plants in Ω_i. This section endeavors to show that any choice of $B(\theta)$ from the set $Co\left\{B\left(\theta_{ij}\right)\right\}$ will work. For ease of exposition fix the subspace Ω_i (i.e. remove index i) and let A be constant in Ω_i. Also use the familiar LQR gains Q, R where in Sec. 4.1 $Q = C_z^T C_z$ and $R = D_z^T D_z$. A successful solution of inequality (4.5) implies

$$A^T P + PA - PB_j R^{-1} B_j^T P - PB_j R^{-1} B_j^T P < -Q, \quad \forall j \tag{4.11}$$

which can also be written

$$A^T P + PA + K^T B_j^T P + PB_j K < -Q, \quad \forall j \tag{4.12}$$

where $K = -R^{-1}B_j^T P$. But for a fixed gain K we need $K = -R^{-1}B_*^T P$ with fixed B_*. The following proposition addresses the choice of B_*. But first consider the scalar case of Eqn. (4.11),

$$2ap + p < 2p^2 b_* b_j / r \tag{4.13}$$

where a p and r can always be found such that Eqn. (4.13) holds unless $b_* b_j$ changes sign. This observation can be generalized to show flexibility in choose of B_*.

Proposition 4.3. *If a P exists to satisfy the j inequalities of Eqn. (4.11), then any $B_* \in Co\{B(\theta_{ij})\}$ can be chosen for the state feedback gain*

$$K = -R^{-1}B_*^T P \tag{4.14}$$

to satisfy inequalities (4.12) with the K of Eqn. (4.14).

Proof. Factor

$$B_* = (\Delta_j + I) B_j \tag{4.15}$$

where the necessary for regulation controllability condition

$$\begin{bmatrix} I & A & A^2 & \dots \end{bmatrix} (\Delta_j + I)^{-1} B_* \tag{4.16}$$

implies $\Delta_j < I$. Let $X = P^{-1}$. Substitute and expand

$$\begin{aligned} B_* R^{-1} B_j^T + B_j R^{-1} B_*^T &> XA^T + AX + XQX \\ (\Delta_j + I) B_j R^{-1} B_j^T + B_j R^{-1} B_j^T \left(I + \Delta_j^T\right) &> \\ B_j R^{-1} B_j^T + B_j R^{-1} B_j^T + \Delta_j B_j R^{-1} B_j^T + B_j R^{-1} B_j^T \Delta_j^T &> \end{aligned} \tag{4.17}$$

The matrix identity $A \geq B$, $C \geq D$, $A + C \geq B + D$ (where $A \geq B \Rightarrow A - B \geq 0$) implies

$$B_j R^{-1} B_j^T + B_j R^{-1} B_j^T > \Delta_j B_j R^{-1} B_j^T + B_j R^{-1} B_j^T \Delta_j^T$$

such that a P, R can always be found to satisfy Eqn. (4.17). □

The above proposition verifies the statement of Sec. 4.2, specifically

Corollary 4.4. *If Eqn. (4.5) holds for all $A(\theta_{ij})$, $B(\theta_{ij})$ and B_i is chosen according to Eqn. (4.7), then a solution P_i of the block LMI*

$$A_{CL}^T(\theta_{ij}) P_i + P_i A_{CL}(\theta_{ij}) + Q_i < 0$$

with $A_{CL}(\theta_{ij}) = A(\theta_{ij}) + B(\theta_{ij}) K_i$ exists.

A note of caution - Proposition 4.3 ensures a P can be found, but it may not be the P obtained from Eqn. (4.5). The designer may need to choose B_i then solve Eqn. (4.8) to obtain P and K. A general guideline is to choose B_i such that $\|K\|_2$ is minimized to improve robustness to unmodeled error. Therefore choose as B_i the matrix $B(\vartheta_{ij})$ that minimizes $\|B(\theta)\|_2$ over $\theta \in \Omega_i$.

4.4 Regulator Type

Now apply Eqn. (4.5) to design the set of controllers $\{C_1, \ldots, C_N\}$ of the multi-model controller in Fig. 1.2. Two types of regulator design are described in [KK78] and only the "Error Augmentation" regulator design method is convex. A "Disturbance Estimation" regulator design is shown to be a Bilinear Matrix Inequality in [PK14] due to the design degrees of freedom of the observer. Error augmentation regulators [Dav72, KK78] use only an explicit copy of the disturbance model Eqn. (1.2) and an observer is not mandatory.

4.4.1 Error Augmentation

The composite plant matrices for use in Eqn. (4.5) are

$$\bar{A}(\theta_{ij}) = \begin{bmatrix} A(\theta_{ij}) & 0 \\ J_i C(\theta_{ij}) & Z \end{bmatrix}, \bar{B}(\theta_{ij}) = \begin{bmatrix} B(\theta_{ij}) \\ 0 \end{bmatrix} \tag{4.18}$$

4.4.2 Disturbance Estimation

Implement state feedback control of Eqn. (2.1) using observed states $\hat{x}$, $\hat{\vartheta}$,

$$u = K \begin{bmatrix} \hat{x} \\ \hat{\vartheta} \end{bmatrix} \tag{4.19}$$

The closed loop dynamics of the plant, exogenous system, and observer are

$$\dot{x}_{cl} = A_{cl} x_{cl}$$

$$e = C_{cl} x_{cl}$$

with state vector

$$x_{cl} = \begin{bmatrix} x & \hat{\tilde{x}} & \vartheta \end{bmatrix} = \begin{bmatrix} x & \hat{x} & \hat{\vartheta} & \vartheta \end{bmatrix}$$

where

$$A_{cl} = \left[\begin{array}{cc|c} A & BK & E \\ -LC & A_o + LC_o + B_o K & -LF \\ \hline 0 & 0 & Z \end{array}\right] \tag{4.20}$$

$$C_{cl} = \begin{bmatrix} C & 0 & F \end{bmatrix}$$

and the composite observer matrices are

$$A_o = \begin{bmatrix} A & E \\ 0 & Z \end{bmatrix}, B_o = \begin{bmatrix} B \\ 0 \end{bmatrix},$$

$$C_o = \begin{bmatrix} C & F \end{bmatrix}, K = \begin{bmatrix} K_x & K_\vartheta \end{bmatrix}.$$

The internal model compensator design requires that the spectrum of Z be contained in the spectrum of the observer dynamics,

$$\sigma(Z) \subset \sigma(A_o + LC_o + B_oK) \tag{4.21}$$

The design parameters are controller gains K, L and observer matrices A_o,B_o,C_o subject to the internal model condition Eqn. (4.21).

Disturbance Estimation Type Regulator as Bilinear Matrix Inequality Let A_{11} be the top left block of the partitioned A_{cl} of Eqn. (4.20). In the case of no state information, A_{11} is dimension $2n + p$. Write A_{11} to account for possible plant (θ) and observer(o) mismatch,

$$A_{11} = \begin{bmatrix} A_\theta & B_\theta K \\ -LC_\theta & \hat{A}_o + L\hat{C}_o + \hat{B}_oK \end{bmatrix}$$

where the composite matrices of the observer $\left\{\hat{A}_o, \hat{B}_o, \hat{C}_o\right\}$ contain estimates $\left\{\hat{A}, \hat{B}, \hat{C}\right\}$ of the true plant matrices $\{A, B, C\}$,

$$\hat{A}_o = \begin{bmatrix} \hat{A} & \hat{E} \\ 0 & Z \end{bmatrix}, \hat{B}_o = \begin{bmatrix} \hat{B} \\ 0 \end{bmatrix}, \hat{C}_o = \begin{bmatrix} \hat{C} & \hat{F} \end{bmatrix}$$

The algebraic Riccati equation

$$A_{11}^T P + P A_{11} < 0 \tag{4.22}$$

is linear in both the independent variable P and design parameters K, L, $\hat{A}_o$, $\hat{B}_o$, $\hat{C}_o$. Hence, Eqn. (4.22) is a Bilinear Linear Matrix Inequality (BLMI). Therefore, regulator design of the disturbance estimation type will not be pursued further in this thesis.

Remark 4.5. *Were the observer model an exact copy of the true plant dynamics, i.e.* $\hat{A} = A_\theta$ *& etc., the separation principle would hold and* A_{11} *could be transformed to an upper triangular form. Then Eqn. (4.2) could be solved for* K_x *in* $\hat{A} + \hat{B}K_x$ *and again for the dual problem of* L *in* $A_o^T + C_o^T L^T$ *. In this idealized case a CQLF is certain for* A_{11} *in upper triangular form.*

The procedure suggested in Remark (4.5) may obtain a CQLF matrix P via Eqn. (4.2), but $\hat{A}$, $\hat{B}$, and $\hat{C}$ are obtained by trial and error.

Consider Remark 4.5 in more detail. Note that matrices A_θ and B_θ have parameters with values in the continuum of the parameter space whereas the observer design matrices $\hat{A}$ and $\hat{B}$ are selected from parameter values fixed in each polytope $\theta_{ij} \in \Omega_i$. Consider a transformation to state and observer error coordinates $\{x, \tilde{x}\}$ where $\tilde{x} = \hat{x} - x$ such that with exact knowledge of plant matrices $\{A, B, C\}$ the separation principle holds and the closed loop dynamics matrix is upper triangular. Transform A_{11} to obtain the closed loop dynamics of $\tilde{x}$ is $\tilde{A}$ where

$$\tilde{A} = \begin{bmatrix} A_\theta + B_\theta K_x & B_\theta K \\ \delta & \hat{A}_o + L\hat{C}_o + \left(\hat{B}_o - B_\theta\right) K \end{bmatrix}$$

and

$$\delta = \begin{bmatrix} \left(\hat{A} - A_\theta\right) + \left(\hat{B} - B_\theta\right) K_x \\ 0 \end{bmatrix}$$

If K and L are designed according to the separation principle, then quadratic stability of $\tilde{A}$ is guaranteed only if $\delta = 0$ for all $\theta \in \Omega$. Since $\hat{A}$ and $\hat{B}$ are constant but A_θ and B_θ vary with θ, in general $\delta \neq 0$. Thus, δ destroys the separation principle, invalidates the CQLF based on K and L, and may even cause instability.

Further insight may be drawn from the characteristic polynomial of the closed loop dynamics matrix A_{11}. Solve for the determinant of $(sI - A_{11})$ in partitioned form using

Schur's formula,

$$\det\left(s-\left(A_\theta+B_\theta K_x\right)\right)\cdot\det\left(s-\left(\hat{A}_o+L\hat{C}_o+\left(\hat{B}_o-B_\theta\right)K\right)-\delta\left(s-\left(A_\theta+B_\theta K_x\right)\right)^{-1}B_\theta K\right) \tag{4.23}$$

or

$$\det\left(s-\left(\hat{A}_o+L\hat{C}_o+\left(\hat{B}_o-B_\theta\right)K\right)\right)\cdot$$
$$\det\left(s-\left(A_\theta+B_\theta K_x\right)-B_\theta K\left(s-\left(\hat{A}_o+L\hat{C}_o+\left(\hat{B}_o-B_\theta\right)K\right)\right)^{-1}\delta\right)$$

Note that Eqn. (4.23) implies K_x can obtained independently of L. Also, since $\left\{\hat{A}_o,\hat{C}_o\right\}$ is controllable the term with δ can be made arbitrarily small by choosing L arbitrarily large. Since the observer contains a copy of the exogenous dynamics model,

$$\sigma\left(Z\right)\subset\sigma\left(\hat{A}_o+L\hat{C}_o+\hat{B}_oK\right)$$

regulation may still proceed despite the loss of common quadratic stability.

5. LONGITUDINAL AIRCRAFT DYNAMICS MODEL

A parameter dependent longitudinal aircraft dynamics model is described in detail. This physical model motivates the results of this thesis. The equations of motion are developed and then analyzed for a one and two parameter model. Lastly a simplified, linear model is developed for use in Chapter 6.

5.1 Equations of Motion

Consider the longitudinal dynamics of a generic aircraft [KBB91]. This system has four states and two outputs ($n = 4$, $p = 2$). The state vector $x = [v,\ \alpha,\ \theta,\ q]^T$ is comprised of velocity v, angle of attack α, pitch θ, and pitch rate q. The system has two inputs ($m = 2$), thrust Π and elevator δ. The a priori unknown parameters are the center of gravity location κ, the commanded velocity v^*, and the commanded flight path angle γ^* where $\gamma = \theta - \alpha$.

The system may be written in the form of Eqn. (1.4) as

$$\begin{aligned} f(x, u, \vartheta) &= R(v, \alpha)^{-1} \cdot M(x, u, \vartheta) \\ h(x, u, \vartheta) &= \{v - v^*, \gamma - \gamma^*\} \end{aligned} \tag{5.1}$$

where the flight path angle is $\gamma = \theta - \alpha$ and v^* and γ^* are the commanded velocity and flight path angle. The equations of motion $M(x, u, \vartheta)$ can be found by ΣF_x, ΣF_z, and ΣM_y about a body fixed axis

$$M(x, u, \vartheta) = \begin{bmatrix} -W \sin\theta - D \cos\alpha + L_w \sin\alpha \\ W \cos\theta - D \sin\alpha - L_w \cos\alpha \\ q \\ c_1 (M_w + \kappa L_w \cos\alpha) - c_2\, q \end{bmatrix} + \begin{bmatrix} \Pi + L_t \sin\alpha_t \\ -L_t \cos\alpha_t \\ 0 \\ -c_1 (1 - \kappa) L_t \cos\alpha_t \end{bmatrix}$$

Application of Lift (L), Drag (D), Weight (W), Thrust (T), and velocity (U) vectors in the $x - z$ plane of symmetry are shown in Fig. 5.1

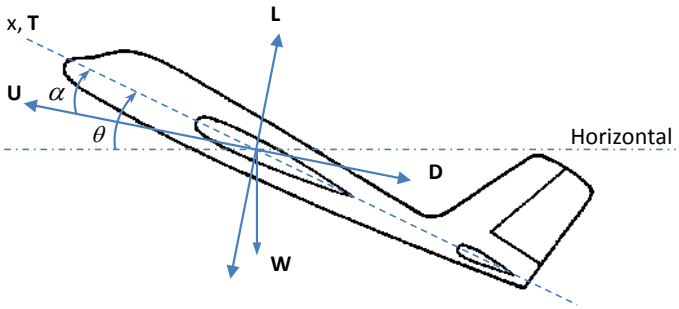

Figure 5.1: Longitudinal State Variables And Partial Free Body Diagram

The rotation from body to wind coordinates $R(v,\alpha)$ is

$$R(v,\alpha) = \begin{bmatrix} \cos\alpha & -v\sin\alpha & v\sin\alpha & 0 \\ \sin\alpha & v\cos\alpha & -v\cos\alpha & 0 \\ 0 & 0 & 1 & 0 \\ 0 & 0 & 0 & 1 \end{bmatrix}$$

The aerodynamic functions are normalized

$$\text{Weight} = W = 1, \qquad \text{Drag} = D = \rho v^2 \left(a + b\, F_w^2\right),$$

$$\text{Lift (wing)} = L_w = \rho v^2 F_w, \qquad \text{Lift (tail)} = L_t = \rho v^2 F_t$$

where lift is cubic in α and elevator δ,

$$\begin{aligned} F_t &= \frac{d}{\alpha_0}\left(\alpha - \alpha_0 + \delta - 3\left(\alpha - \alpha_0 + \delta\right)^3\right) \\ F_w &= \frac{1}{\alpha_0}\left(\alpha - 2.08\left(\alpha - \alpha_0\right)^3\right) \end{aligned}$$

$$\alpha_t = \alpha + \delta,\ \alpha_0 = \tfrac{1}{20},\ a = \tfrac{1}{20}, b = \tfrac{1}{20},\ c_1 = 300,\ c_2 = 8,\ d = \tfrac{1}{10}$$

with $\rho = 1$ and a wing moment M_w of zero. Envelope and actuator and parameter constraints are as follows. Note that only level flight is considered here. Velocity is normalized

by maximum cruise velocity.

$$0 \leq v \leq 1,\ -0.5 \leq \delta \leq 0.5\ 0 \leq \Pi \leq 1 \tag{5.2}$$

$$0.5 \leq v^* \leq 1,\ \gamma^* = 0,\ 0 \leq \kappa \leq 0.2 \tag{5.3}$$

5.2 Linear Family of Plants

5.2.1 Parameter Dependent Systems

Consider feedback regulation of the parameter dependent, nonlinear system Eqn. (1.4) with known disturbance dynamics Eqn. (1.2). Recall that $Z = 0_k$ since only constant disturbances and set-points are permitted in this thesis. The family of plants, and hence the subfamilies of plants with equivalent zero structure, vary with ϑ.

Regulation suggests a stable equilibrium such that $e \to 0$ as $t \to \infty$. The equilibrium surface $\mathcal{E}^*$ is the set of points (x, u, ϑ) invariant under dynamics Eqn. (1.4) for which regulation succeeds,

$$\mathcal{E}^* = \{(x, u, \vartheta) \,|\mathcal{E}\,(x, u, \vartheta) = 0\} \tag{5.4}$$

where the function $\mathcal{E} : R^{n+m+k} \to R^{n+p}$ is defined as

$$\mathcal{E}\,(x, u, \vartheta) \equiv \begin{bmatrix} f\,(x, u, \vartheta) \\ h\,(x, \vartheta) \end{bmatrix}.$$

A family of parameter dependent, linear plants $\mathcal{P}$ is obtained by Taylor linearization of system Eqn. (1.4) on the equilibrium surface $\mathcal{E}^*$.

Definition 5.1. *Each plant in the family of plants,* $\mathbf{p}(\vartheta) \in \mathcal{P}$*, is the regulator problem*

$$\begin{aligned} \dot{x} &= A(\vartheta)\, x + B(\vartheta)\, u + E(\vartheta)\, \vartheta \\ \dot{\vartheta} &= Z\vartheta \\ e &= C(\vartheta)\, x + F(\vartheta)\, \vartheta \end{aligned} \tag{5.5}$$

whose construction is detailed below.

Plant matrices A, B, C, E, and F are the partial derivatives evaluated at an equilibrium point (x^*, u^*, ϑ^*), e.g.

$$A = \frac{\partial}{\partial x}\, f(x, u, \vartheta)|_{x^*, u^*, \vartheta^*}, \text{ etc.}$$

The equilibrium surface is an implicit manifold of dimension k since Eqn. (5.4) is $n + m + k$ variables with $n + p$ constraint equations (per Section 2.1, $m = p$ for square systems). Hence the set $\{A(\vartheta), B(\vartheta), C(\vartheta), E(\vartheta), F(\vartheta)\}$ are uniquely defined by k parameters. Parameterization of the equilibrium manifold is illustrated in Example 7.2.

Robust regulation with continuous state feedback control $u = K(x, \vartheta)$ is considered in this paper. Hence, $\{A(\vartheta), B(\vartheta), C(\vartheta)\}$ must be smooth in the parameter ϑ. Specifically, the system matrix Γ must be full rank such that Eqn. (5.4) can be solved for any $\{E, F\}$ in an open neighborhood of $\mathcal{E}^*$ as detailed in Section 2.3.

The parameter dependent linearized system may be written

$$\begin{aligned} \delta\dot{x} &= A(\vartheta)\, \delta x + B(\vartheta)\, \delta u + E(\vartheta)\, \delta\vartheta \\ \delta e &= C(\vartheta)\, \delta x + F(\vartheta)\, \delta\vartheta \end{aligned} \tag{5.6}$$

Then obtain each $p(\vartheta)$ in (5.5) by joining the disturbance model (1.2) to (5.6).

If the plant is a linear system with linear parametric uncertainty, i.e. the $A(\vartheta)$, etc. are linear in ϑ, the plant family is convex in ϑ. Multiple Model Adaptive Regulation for this case is presented in Chapter 6.

In the general nonlinear system, the exogenous disturbances and parametric uncertainty are lumped together as discussed in Sec. 1.2.1 and Example 1.1. Multiple Model Adaptive Regulation for this case is presented in Chapter 7.

5.3 Plant Properties

A quantitative analysis of the linear family of plants along a one parameter (1-D) is tabulated below. A qualitative analysis of the two parameter (2-D) equilibrium surface is then illustrated.

5.3.1 One Parameter Equilibrium Surface

When the velocity v^* and flight path angle γ^* commands are known the equilibrium constraint $\mathcal{E} = 0$ is $n + p = 6$ equations with $n + m + k = 7$ variables and the equilibrium surface has dimension one. The one dimensional equilibrium surface is plotted in Fig. 5.2 in cartesian coordinates (κ, δ). Equilibrium values for the elevator angle δ as a function of κ at a fixed velocity and level flight trim condition $(v^*, \gamma^*) = (0.5, 0)$ are shown in Fig. 5.2. Only the portion of the equilibrium curve below the red dot on the bottom branch at $\kappa \approx 0.057$ is open loop stable. As shown in Table 5.1, the $B_{4,2}$ matrix element changes sign at the singular surface which is the nose of the curve where the two branches of the equilibrium surface meet. The two branches meet at approximately $\kappa = 0.12$ and vanish for $\kappa > 0.12$.

The following properties of linearized plants in $\mathcal{E}^*$ are explored in more detail:

- State space representation
- State, control, and force values
- Open loop properties including poles and transmission zeros

A table of open loop properties for a subset of the plants on the equilibrium surface pictures in Fig. 5.2 is provided in Table 5.3 in Section 5.3.1 below.

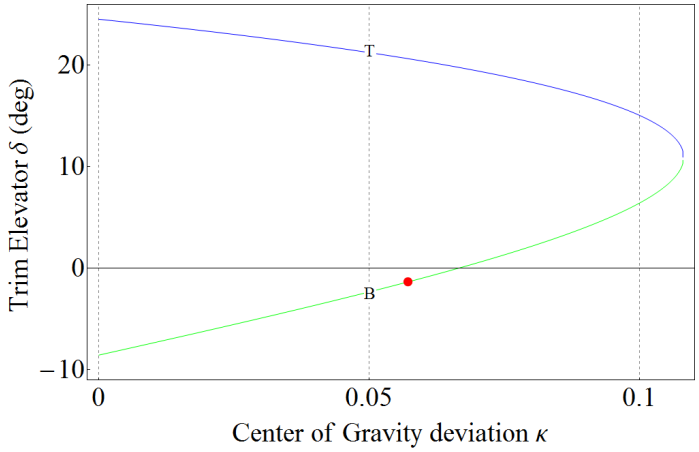

Figure 5.2: Equilibrium Curve δ vs. κ at Fixed Velocity

State Space Elements

The system has a natural state space representation with state vector $x = [v,\ \alpha,\ \theta,\ q]^T$. The parameter dependent A and B matrices for the natural state space representation are

$$A = \begin{bmatrix} a_{11} & a_{12} & -1 & 0 \\ a_{21} & a_{22} & 0 & 1 \\ 0 & 0 & 0 & 1 \\ 0 & a_{42} & 0 & -8 \end{bmatrix},\ B = \begin{bmatrix} b_{11} & b_{12} \\ b_{21} & b_{22} \\ 0 & 0 \\ 0 & b_{42} \end{bmatrix} \tag{5.7a}$$

and C is parameter free

$$C = \begin{bmatrix} 1 & 0 & 0 & 0 \\ 0 & -1 & 1 & 0 \end{bmatrix} \tag{5.7b}$$

Coefficients that vary along the equilibrium surface are represented by a_{ij} and b_{ij}. Values for a_{ij} and b_{ij} are given in Table 5.1. This table is computed along a line of constant velocity $v = 0.5$. The equilibrium sheet is denoted by B and T for bottom and top respectively. Values of κ have been selected to show loss of open loop stability and loss of simultaneous regulation.

State, Control, & Aerodynamic values

Values for the state, control, and aerodynamic forces for the 1-D equilibrium curve shown in Fig. 5.2 are collected in Table 5.2. Values for three of the four states are known,

- $v = 0.5$ as specified
- $q = 0$ since $\dot{\theta} = 0$
- $\theta = \alpha$ since $\gamma = \theta - \alpha$ & $\gamma = 0$

The remaining state α, the controls Π and δ, and the magnitude of the aerodynamic forces Drag and wing and tail Lift are tabulated in Table 5.2. Open loop stability is lost when $\dfrac{\partial \dot{q}}{\partial \alpha}$ changes sign as shown by element a_{42}; Simultaneous regulation is lost when $\dfrac{\partial \text{Lift}_{Tail}}{\partial \delta}$ as shown by element b_{42} in Table 5.1.

The angle of attack α is relatively constant (with $v = 0.5$), but the tail angle of attack α_{Tail} increases as $\mathcal{E}^*$ is traversed in Table 5.2. The drag and hence thrust is minimal near the inflection point in the equilibrium curve, making this an attractive trim condition for fuel savings. The elevator deflection also increases as $\mathcal{E}^*$ is traversed. All equilibrium points shown in the table are feasible for an aircraft in normal operating condition.

Open Loop Analysis

Open loop system properties for the set of plants along the equilibrium curve in the following table shows the change in system properties along a line of constant velocity $v = 0.5$.

The transmission zero polynomial is obtained by $\det \Gamma(\lambda)$. The roots (i.e. zeros) are relatively constant over the equilibrium curve. The zero polynomial changes rapidly near the singular surface. Note that the constant term in the zero polynomial is the $\det \Gamma$.

Table 5.3 shows the change in state α, control inputs Π and δ, and the zero polynomial and poles of plants as a function of κ while velocity is held constant at $v = 0.5$. The bottom and top equilibrium sheets roughly correspond to low and high elevator deflection.

The first entry in the table at $\kappa = 0$ on the bottom equilibrium sheet shows the traditional short period and phugoid modes. Stability is first lost at approximately $\kappa = 0.57$ on the bottom equilibrium sheet. The eigenvalues are stable for a portion of the bottom equilibrium sheet but are unstable for all of the top equilibrium sheet.

5.3.2 Two Parameter Equilibrium & Singular Surface

Kappa, Delta, Velocity

When only the flight path angle command γ^* is known the equilibrium constraint $\mathcal{E} = 0$ is $n+p = 6$ equations with $n+m+k = 8$ variables and the equilibrium surface has dimension two. The equilibrium equation $\mathcal{E}(x, u, \vartheta) = 0$ may be solved by noting that $q = 0$ at steady state and specifying v^* such that κ is the independent variable; thus $\mathcal{E}$ is reduced to three equations in variables α, Π, δ. Repeat this process over the domain of $\{v^*, \kappa\}$ in Eqn. (5.3) to form a set of points $\mathcal{E}^*$ per Eqn. (5.4).

The two dimensional equilibrium surface is plotted in Fig. 5.3 in coordinates (κ, v, δ) as the unshaded mesh. The shaded portions of the mesh equilibrium surface correspond to control covering as described in Sec. 7.3.1. The portion of the equilibrium sheet below the dashed red line is open loop stable. Whereas the 1-D equilibrium curve has branches, the disjoint sets of the 2-D equilibrium surface will be called sheets. In this example, the top and bottom sheets of the equilibrium surface may be distinguished by the sign of $\det \Gamma$ in Eqn. (2.11). The surface area of the top equilibrium sheet of Fig. 5.3 is smaller than the bottom equilibrium sheet due to enforcement of constraints Eqn. (5.2).

Kappa, Delta, Alpha

By judicious choice of elimination of variable, a contour plot of the equilibrium and singular surfaces can be generated. Assume γ^* is known while v^* and κ is not known. Thus there are $n + 1 = 5$ constraint equations and $n + m + k = 7$ unknowns for a 2-D equilibrium surface. First obtain a singular surface contour plot:

Table 5.1: Variation in State Space Coefficients for Equilibrium Curve of Fig. 5.2

κ	Sheet	a_{11}	a_{12}	a_{21}	a_{22}	a_{42}	b_{11}	b_{12}	b_{21}	b_{22}	b_{42}
0.	B	−0.79	−0.77	−7.7	−10.	−150.	0.98	−0.07	−0.4	−0.99	−150.
0.05	B	−0.73	−0.67	−7.7	−10.	−64.	0.98	0.03	−0.38	−0.92	−127.
0.075	B	−0.68	−0.61	−7.7	−10.	−6.7	0.98	0.08	−0.37	−0.77	−101.
0.108	B	−0.57	−0.57	−7.8	−9.4	131.	0.98	0.12	−0.35	−0.1	−7.6
0.108	T	−0.56	−0.58	−7.8	−9.3	146.	0.98	0.11	−0.35	0.02	7.7
0.075	T	−0.58	−0.77	−7.8	−8.3	219.	0.98	−0.08	−0.37	0.94	125.
0.05	T	−0.64	−0.89	−7.8	−7.9	233.	0.98	−0.19	−0.38	1.3	170.
0.	T	−0.79	−1.1	−7.7	−7.2	243.	0.98	−0.42	−0.4	1.8	243.

Table 5.2: Variation in Inputs, States, & Aerodynamic Forces for Equilibrium Curve of Fig. 5.2

κ	Sheet	δ	Π	α	α_{Tail}	Drag	Lift$_{Wing}$	Lift$_{Tail}$
0.	B	−0.15	0.2	0.2	0.05	0.2	0.96	0.
0.05	B	−0.04	0.19	0.19	0.15	0.18	0.92	0.05
0.075	B	0.02	0.17	0.18	0.21	0.17	0.9	0.07
0.108	B	0.18	0.14	0.18	0.36	0.16	0.87	0.11
0.108	T	0.2	0.14	0.18	0.38	0.16	0.87	0.11
0.075	T	0.33	0.15	0.18	0.51	0.17	0.9	0.08
0.05	T	0.37	0.16	0.19	0.56	0.18	0.92	0.06
0.	T	0.43	0.2	0.2	0.63	0.2	0.96	0.

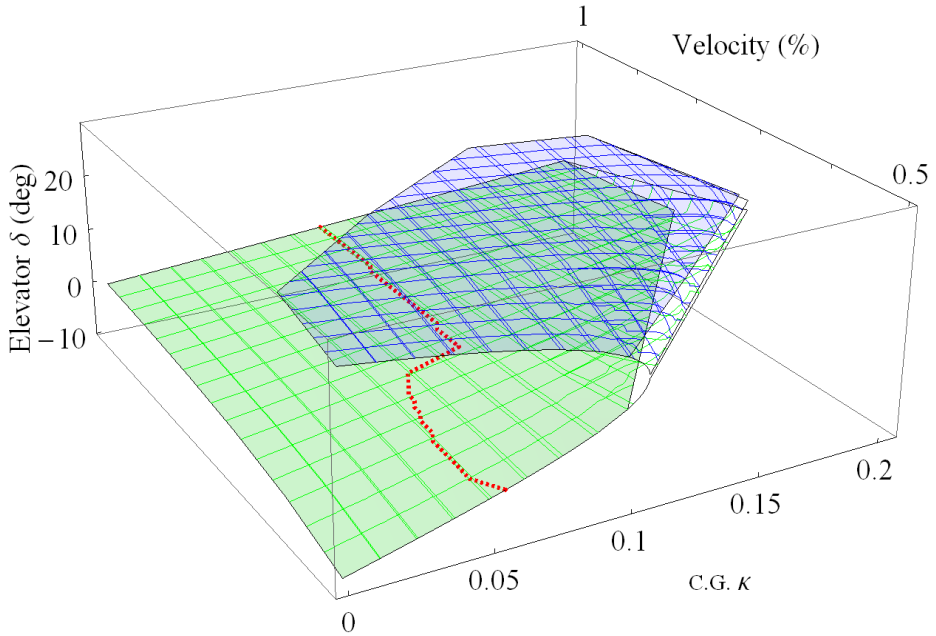

Figure 5.3: Equilibrium Sheets

κ	Sheet	$\det\Gamma$	zero polynomial	λ_1	λ_2	λ_3	λ_4
0.	B	$-1423.$	$1.\lambda^2 + 8.\lambda - 1423.$	$-9. + 12.i$	$-9. - 12.i$	$-0.1 + 2.2i$	$-0.1 - 2.2i$
0.05	B	$-1274.$	$0.89\lambda^2 + 7.1\lambda - 1274.$	$-9. + 8.i$	$-9. - 8.i$	$-0.01 + 1.8i$	$-0.01 - 1.8i$
0.075	B	$-1050.$	$0.73\lambda^2 + 5.8\lambda - 1050.$	$-9.3 + 2.3i$	$-9.3 - 2.3i$	$-0.06 + 0.75i$	$-0.06 - 0.75i$
0.108	B	$-82.$	$0.06\lambda^2 + 0.45\lambda - 82.$	$-20.$	4.8	$-1.2 + 3.i$	$-1.2 - 3.i$
0.108	T	83.	$-0.06\lambda^2 - 0.46\lambda + 83.$	$-21.$	5.3	$-1.1 + 3.i$	$-1.1 - 3.i$
0.075	T	1295.	$-0.9\lambda^2 - 7.2\lambda + 1295.$	$-23.$	7.9	$-0.8 + 3.i$	$-0.8 - 3.i$
0.05	T	1716.	$-1.2\lambda^2 - 9.6\lambda + 1716.$	$-23.$	8.5	$-0.8 + 2.9i$	$-0.8 - 2.9i$
0.	T	2308.	$-1.6\lambda^2 - 13.\lambda + 2308.$	$-23.$	9.1	$-0.8 + 2.8i$	$-0.8 - 2.8i$

Table 5.3: Variation in system properties along Equilibrium Curve of Fig 5.2

1. Note that $q = 0$ at equilibrium and solve $\gamma \equiv \theta - \alpha$ for θ as a function in α
2. Solve $\dot{v}(x, u, \kappa) = 0$ & $\dot{\alpha}(x, u, \kappa) = 0$ for Π & v as functions in (κ, α, δ)
3. Evaluate partial derivatives to obtain exact equations for $A = \frac{\partial}{\partial x} f(x, u, \vartheta)$, $B = \frac{\partial}{\partial u} f(x, u, \vartheta)$, $C = \frac{\partial}{\partial x} h(x, u, \vartheta)$. Then apply above substitutions for $\{q, \theta, v, \Pi\}$ to form Γ from these $\{A, B, C\}$
4. Set $\det \Gamma = 0$ and plot this one equation in the remaining three variables (κ, α, δ)

Now obtain the equilibrium surface contour plot:

1. Steps 1 & 2 above.
2. set $\dot{q}(x, u, \kappa) = 0$ and plot this one equation in the remaining three variables (κ, α, δ)

Contour plots of the equilibrium and singular surfaces are combined in Fig. 5.4. Note that regulation of plants away from the equilibrium surface will suffer loss of regulation. A nonlinear regulator valid over the region shown will need to accommodate the loss of simultaneous regulation. The singular surface may not be exact due to numerical issues while clearing fractions for variable elimination.

5.4 Simplified Model

5.4.1 SISO System

The states x_1, x_2, and x_3 approximate angle of attack, pitch, and pitch rate respectively. The angle of attack has relative degree one and the zero structure of pitch & pitch rate is preserved. The zero structure changes with operation at low and high angles of attack. The derivation of the simplified model is explored in greater detail in Sec. 5.4.2 below.

Consider a system with state vector $x^T = \begin{bmatrix} x_1 & x_2 & x_3 \end{bmatrix}$ and parameter dependent

state space representation,

$$A = \begin{bmatrix} \theta_1 & 0 & 1 \\ 0 & 0 & 1 \\ \theta_2 & 0 & \theta_3 \end{bmatrix}, B = \begin{bmatrix} 1 \\ 0 \\ 0 \end{bmatrix}, C = \begin{bmatrix} 1 & 1 & 0 \end{bmatrix}, D = 0 \tag{5.8}$$

The reference input and state disturbance are constant signals such that $Z = 0$ in Eqn. (1.2) and enter as

$$F = -1,\ E^T = \begin{bmatrix} 0 & 0 & 1 \end{bmatrix} \tag{5.9}$$

Here θ_1, θ_2 and θ_3 are unknown but constant parameters. The transfer function

$$T(s) = C(sI - A)^{-1} B$$

is

$$T(s) = \frac{s^2 - s\theta_3 + \theta_2}{s(s^2 - s(\theta_1 + \theta_3) - \theta_2 + \theta_1\theta_3)}$$

When $\theta_2 = 0$ the system is structurally unstable with

- a transmission zero at $s = 0$,
- a pole at the origin,
- (A, B) is uncontrollable

Parameter variation for the damping terms are

$$-5 \leq \theta_1 \leq -4,\ -5 \leq \theta_3 \leq -4$$

The two subfamilies (top & bottom) are a function of θ_2 and may be defined by the sign of $\det \Gamma_\theta$.

$$\det \Gamma_\theta(0) = \begin{cases} > 0 & \text{Top: } \theta_2 \in [-4, -1] \\ < 0 & \text{Bottom: } \theta_2 \in [1, 4] \end{cases} \tag{5.10}$$

The two subfamilies are shown in the parameter space in Fig. 5.5.

5.4.2 Derivation of the Simplified Model

To facilitate development of control strategies a linear, SISO abstraction of the nonlinear, MIMO longitudinal aircraft dynamics of Eqn. (5.1) was derived. Development of the abstracted model is detailed in this section. The zero structure change of the parameter dependent MIMO system must be retained in the SISO system. The transmission zero polynomial is

$$C_1 s^2 + 8C_1 s - (b_{42}C_2 + a_{42}C_1) \tag{5.11}$$

where

$$C_1 = -(b_{11}b_{22} - b_{12}b_{21})$$

$$C_2 = a_{22}b_{11} + b_{21} - a_{12}b_{21}$$

and the a_{ij}, b_{ij} are defined in Eqn. (5.7a).

When the constant term of Eqn. (5.11) changes sign a zero transits the origin. Hence, variation in state space elements b_{42} and a_{42} is examined.

Consider the four SISO transfer functions of the longitudinal aircraft dynamics model:

$$\begin{bmatrix} v \\ \gamma \end{bmatrix} = \begin{bmatrix} T_{11} & T_{12} \\ T_{21} & T_{22} \end{bmatrix} \begin{bmatrix} \Pi \\ \delta \end{bmatrix}$$

Recall that the zeros of the transfer function elements T_{ij}, $i, j \in \{1, 2\}$ may be unrelated to the transmission or multivariable zeros. For this example the individual transfer function elements have a much richer set of behavior than one sign change at the singular surface. The transfer function $\gamma = T_{12}\Pi$ changes sign when the state space element a_{42} change sign. For the MIMO system the control input element b_{42} change sign at the singular surface, but here the offending parameter is in the A matrix. The parameter values θ_i, $i \in \{1, 2, 3\}$ are approximate values for the system near the change in zero structure.

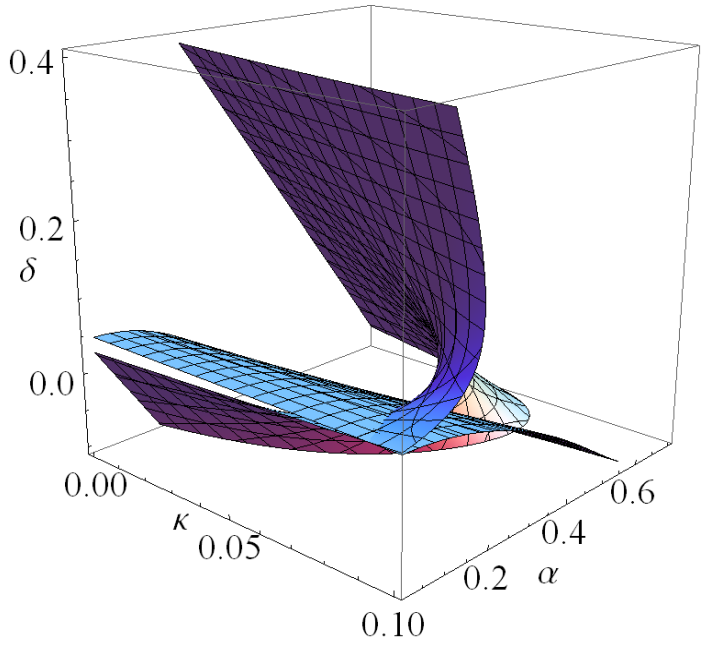

Figure 5.4: Equilibrium and Singular Surfaces

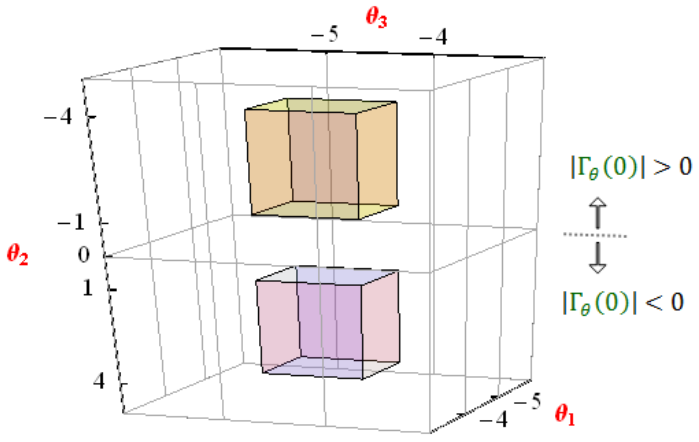

Figure 5.5: Example Problem Parameter Space with Two Subfamilies

Also note that the MIMO system is affine in control in Π but is not affine in δ. Thus, for a jammed (i.e. fixed) elevator the system can be written in the form

$$\dot{x} = f(x) + g(x)\,\Pi$$

This fixed elevator, affine system is used in [KBB91]. Control design for nonlinear systems often assumes this affine form [Isi95, KB00] instead of the more general form of Eqn. (1.4).

6. MMAR FOR LINEAR SYSTEMS

6.1 Regulator Design

The covering and switching design subproblems are solved for the linear SISO system Eqn. (5.8), which is repeated here for convenience,

$$A = \begin{bmatrix} \theta_1 & 0 & 1 \\ 0 & 0 & 1 \\ \theta_2 & 0 & \theta_3 \end{bmatrix}, \; B = \begin{bmatrix} 1 \\ 0 \\ 0 \end{bmatrix}, \; C = \begin{bmatrix} 1 & 1 & 0 \end{bmatrix}, \; D = 0 \qquad \text{(5.8 revisited)}$$

6.1.1 Covering

The subfamilies with similar zero structure are identified in Eqn. (5.10). The top and bottom sheets are defined by the sign of the determinant of Γ_θ.

Let the minimum and maximum value for each parameter θ_{k} be $\underline{\theta}_{\mathsf{k}}$ and $\bar{\theta}_{\mathsf{k}}$ respectively. For k parameters there are 2^k combinations. For this example the two extrema of three parameters form eight combinations. The eight combinations, equivalent to the vertices of a three dimensional rectangle, are listed in Table 6.1 for convenience. The values for the extrema taken from Sec. 5.4.1 are given in Table 6.2.

There are two regions, Ω_i, $i \in \{B, T\}$ with eight vertices per region, $j \in \{1, \ldots, 8\}$.

Example polytopes in two dimensions are shown in Fig. 3.1(Right). In this example, each polytope contains exactly the parameter space of each subfamily.

Form the set of sixteen plant matrices $\left\{ \bar{A}\left(\theta_{ij}\right), \bar{B}\left(\theta_{ij}\right) \right\}$ per Eqns. (4.18) with θ_{ij}, $i \in \{B, T\}$ and $j \in \{1, \ldots, 8\}$. Choose $J_i = 1$ for all i. The $B\left(\theta_{ij}\right)$ and $C\left(\theta_{ij}\right)$ are constant and only $A\left(\theta_{ij}\right)$ varies with i, j. The internal model has dimension of the output ($p = 1$) such

Vertex	Parameter θ_1	Parameter θ_2	Parameter θ_3
1	$\underline{\theta}_1$	$\underline{\theta}_2$	$\underline{\theta}_3$
2	$\bar{\theta}_1$	$\underline{\theta}_2$	$\underline{\theta}_3$
3	$\underline{\theta}_1$	$\bar{\theta}_2$	$\underline{\theta}_3$
4	$\bar{\theta}_1$	$\bar{\theta}_2$	$\underline{\theta}_3$
5	$\underline{\theta}_1$	$\underline{\theta}_2$	$\bar{\theta}_3$
6	$\bar{\theta}_1$	$\underline{\theta}_2$	$\bar{\theta}_3$
7	$\underline{\theta}_1$	$\bar{\theta}_2$	$\bar{\theta}_3$
8	$\bar{\theta}_1$	$\bar{\theta}_2$	$\bar{\theta}_3$

Table 6.1: Polytope vertices θ_{ij}, $j = \{1 \dots 8\}$ for region Ω_i of the SISO example Eqn. (5.8).

Parameter	Parameter Range $[\underline{\theta}, \overline{\theta}]$
θ_1	$[-5, -4]$
θ_2	$[1, 4]$ (Bottom)
	$[-4, -1]$ (Top)
θ_3	$[-5, -4]$

Table 6.2: Parameter range for the SISO example Eqn. (5.8)

that $Z = 0$. Let the LQR design weights of Eqn. (4.1) be

$$\begin{bmatrix} C_z & D_z \end{bmatrix} = \begin{bmatrix} Q_z & 0 \\ 0 & R_z \end{bmatrix} \tag{6.1}$$

where for both subfamilies

$$Q_z = \tfrac{1}{10}\, diag\left([1\ 1\ 25\ 25]\right),\ R_z = 1$$

Now solve the block LMI Eqn. (4.5) comprised of eight inequalities Eqn. (4.2) for both the Bottom and Top subfamilies.

Matlab code to form inequalities Eqn. (4.2), concatenate them into a block LMI Eqn. (4.5) and solve the block LMI with the semidefinite solver YALMIP [Löf04] is included in Appendix B.

Form K_i from Eqn. (4.6) and plant matrices Eqn. (5.8). The solutions for P_B, P_T and K_B, K_T are shown in Table 6.3.

The solutions for K_i are verified if the $A_{CL}\left(\theta_{ij}\right)$ of Eqn. (4.9) have eigenvalues in the closed left half plane. The solutions for P_i are verified if the inequalities Eqn. (4.8) are true for any $Q > 0$.

6.1.2 Switching

The switch logic of Sec. 3.2 requires a Lyapunov function matrix P and the final state x_f. The Lyapunov function matrix is obtained in the preceding section. The final state, x_f is a function of the plant parameters, controller gains, and the disturbance state. For (A, B, C) from Eqn. (5.8), E & F from Eqn. (5.9), state vector $x = [x_1,\ x_2,\ x_3,\ \eta]^T$, feedback gain $K = [k_1,\ k_2,\ k_3,\ k_4]$, and set point ϑ,

$$x_f = \begin{bmatrix} -\frac{\vartheta}{\theta_2} & \vartheta\left(-1 + \frac{1}{\theta_2}\right) & 0 & \frac{\vartheta(\theta_1 + k_1 + k_2(-1+\theta_2))}{k_4\theta_2} \end{bmatrix}^T \tag{6.2}$$

A priori knowledge of the final state x_f is an undesirable feature of this generalized energy (Lyapunov) switch logic as detailed in Sec. 3.2.2.

Assuming the Lyapunov switch logic occurs in software, a sample frequency for evaluating the switch inequalities must be chosen. A slow sample frequency, i.e. large period dt in Eqn. (3.7), improves the signal to noise ratio of the Lyapunov function logic. A fast sample frequency, i.e. small dt, may disproportionately weight high frequency modes. A fast sample frequency results in the switch threshold of Eqn. (3.8) closer to one such that the inequality of Eqn. (3.7) is less obvious, thus resulting in erroneous switches. When dt is large the slow dynamics may inform the switch logic, the inequalities of Eqn. (3.7) are more obvious (better S/N), but model identification may take longer.

A prerouted switch logic [AM02] is acceptable when the cardinality of $\mathcal{C}$ is small.

6.2 Simulation

The multiple model adaptive regulation system was simulated in Mathematica.

Let θ^*, σ^* be the "true" values for the parameter and switch logic index respectively. Set

$$\theta^* = (\theta_1^*, \theta_2^*, \theta_3^*) = (-4, 1, -4)$$

such that $P(\theta^*) \in \Omega_B$ and $\sigma^* = B$. Initialize the plant (x), controller (η), exogenous disturbance (ϑ), and switch logic index (σ) states

$$\begin{aligned} [x_1(0)\ x_2(0)\ x_3(0)\ \eta(0)] &= \begin{bmatrix} 1 & 0 & 0 & 0 \end{bmatrix} \\ \vartheta(0) &= -0.5 \\ \sigma(0) &= T \end{aligned}$$

Initialize the switch logic index $\sigma(t)$ to the top subfamily $\sigma(0) = T$.

Observe in Fig. 6.1(a,b) that the time rate of change of the Lyapunov function $\left(\dot{V}\right)$ immediately ceases to be negative definite (approximately $t = 0.02$). Switching is fast and

accurate as seen in Fig. 6.1(c) where the "Bottom" controller is switched on (i.e. $\sigma = B$) at approximately $t = 0.03$ since the the "wrong" controller (i.e. $\sigma = T$) is not Lyapunov stable.

Output regulation $\lim_{t\to\infty} e(t) = 0$ succeeds as shown in Fig. 6.2(b). The bounded Lyapunov functions V_i, $i \in \{B, T\}$, shown in Fig. 6.1(a) and the system states shown in Fig. 6.2(a) verify internal stability.

Evaluate the final state Eqn. (6.2) to give

$$x_f = \begin{bmatrix} 0.5 & 0 & 0 & -1.38 \end{bmatrix}^T$$

as verified in Fig. 6.2(a).

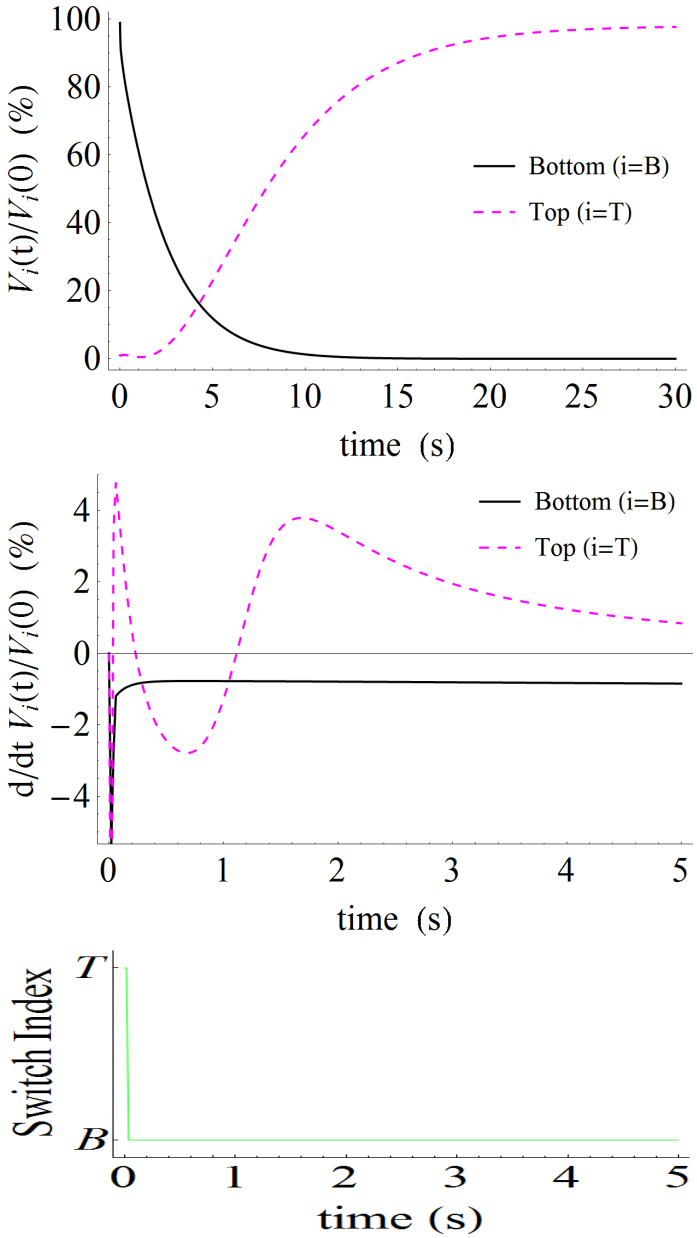

Figure 6.1: MMAR SISO Simulation, Top to bottom: (a) Normalized Lyapunov Function $V_i(t)/V_i(0)$ (%); (b) Normalized Lyapunov time derivative $\frac{d}{dt}V_i(t)/V_i(0)$; (c) Switch index σ

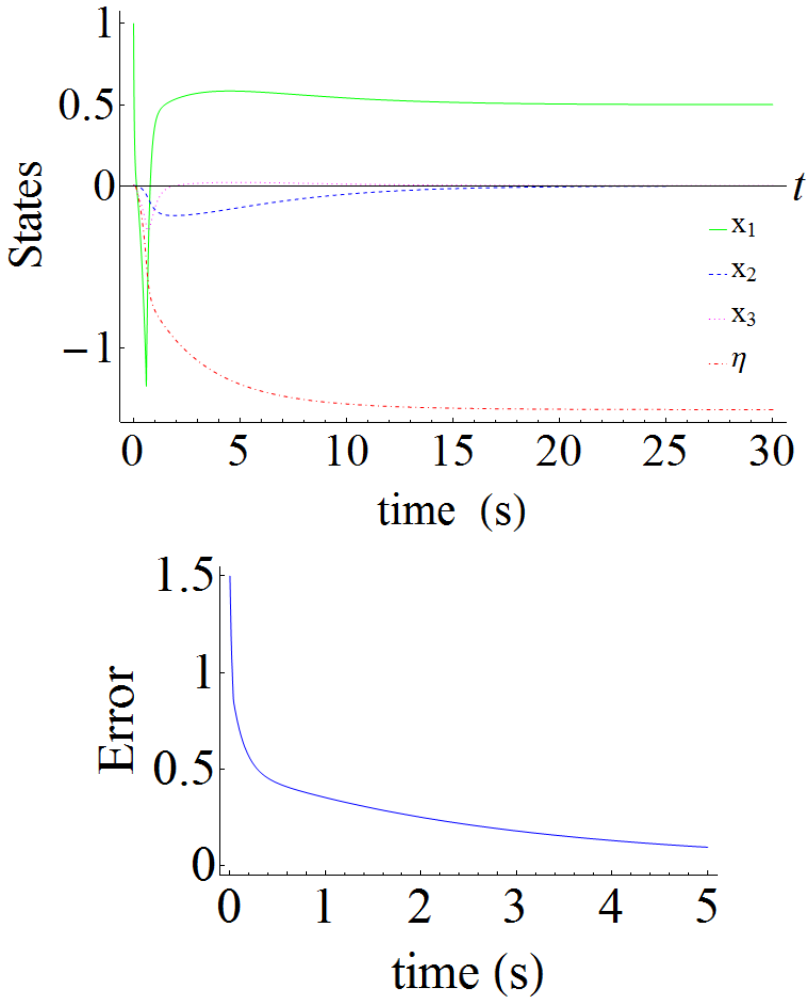

Figure 6.2: MMAR SISO Simulation, Top to Bottom: (a) Plant & Regulator states; (b) Regulation error e

	Equilibrium Sheet	
	Bottom	Top
P_i	$\begin{bmatrix} 3.5 & 8.1 & 2.6 & 2.7 \\ 8.1 & 74. & 18. & 10. \\ 2.6 & 18. & 6.3 & 1.8 \\ 2.7 & 10. & 1.8 & 16. \end{bmatrix}$	$\begin{bmatrix} 18. & -174. & -39. & -25. \\ -174. & 8224. & 1736. & 1230. \\ -39. & 1736. & 389. & 259. \\ -25. & 1230. & 259. & 202. \end{bmatrix}$
K_i	$\begin{bmatrix} -3.5 & -8.2 & -2.6 & -2.7 \end{bmatrix}$	$\begin{bmatrix} -17.6 & 174 & 38.8 & 25.0 \end{bmatrix}$

Table 6.3: Lyapunov (P_i) and LQR (K_i) for SISO example

7. MMAR FOR LINEARIZED SYSTEMS

Whereas Chapter 6 provides an example of Multiple Model Adaptive Regulation for parameter dependent linear systems,

$$\begin{aligned} \dot{x} &= A(\theta)\, x + B(\theta)\, u + E\vartheta \\ y &= C(\theta)\, x + F\vartheta \end{aligned}$$

this chapter provides an example of MMAR for a linear family of plants formed by linearization on the equilibrium surface of parameter dependent, autonomous nonlinear systems

$$\begin{aligned} \dot{x} &= f(x, u, \vartheta) \\ y &= h(x, \vartheta) \end{aligned}$$

The linearization procedure is detailed in Sec. 5.2.1. Application of the MMAR design results of Chapter 4 to these "linearized" systems is detailed in this chapter. The longitudinal aircraft dynamics of Chapter 5 are used to illustrate these results.

As shown in Example 1.1 in Chapter 1, a parameter dependent nonlinear system presents new challenges for regulator design. The results Sec. 4.1 and Sec. 4.2 of Chapter 4 remain the same. Unfortunately a concise accounting of the family of plants with polytopes in the parameter space is no longer feasible. Thus Sec. 4.3 must be modified as follows.

7.1 Plant Linearization

A CQLF is obtained for a region Ω_i in Sec. 4.2, but the region Ω_i has not yet been defined. For a family of plants linear in the unknown parameters, region Ω_i is a polytope defined by vertices $\{\vartheta_{ij}\}$. For a family of plants not linear in the unknown parameters, the demarcation of region Ω_i may require a large set of points $\{\vartheta_{ij}\}$.

Since simultaneous regulation is dependent on the open loop zero structure, and the zero structure is completely described by the system matrix Γ consider the parameter dependence of Γ for linear and nonlinear systems:

- For the linear system Eqn. (1.1) with map $\theta \to \Gamma(\theta)$ linear in θ, the plant matrices $\{A(\theta), B(\theta), C(\theta)\}$ of each $\{\mathbf{p}(\theta) | \theta \in \Omega_i\}$ are convex in θ.

- For the general nonlinear system Eqn. (1.4) with map $\vartheta \to \Gamma(\vartheta)$ continuous in ϑ, the plant matrices $\{A(\vartheta), B(\vartheta), C(\vartheta)\}$ of each $\{\mathbf{p}(\vartheta) | \vartheta \in \Omega_i\}$ may not be convex in ϑ. For example, the tangent manifold of a nonlinear system is not a convex function of the state in general, regardless of the parameter dependence.

Example 7.1. *The dynamics of a parameter dependent nonlinear system are not convex in the parameter in general. This example shows how an affine disturbance affects the convexity of nonlinear systems. Example 1.1 shows how an affine disturbance affects the stability of a nonlinear system. Recall that an affine disturbance has no affect on the stability or convexity of robust regulation of a linear system. Consider a scalar system*

$$\dot{x} = f(x, \vartheta) = -(d(x) + \vartheta) \tag{7.1}$$

where $d(x)$ is a nonlinear function of x. The equilibrium surface is $d(x) + \vartheta = 0$. The system is affine in the parameter ϑ. The design method presented in Chap. 4 is concerned with the convexity of Γ with respect to unknown parameters. Consider the tangent manifold of Eqn. (7.1) parameterized in ϑ

$$A(\vartheta) = \left.\frac{\partial f(x, \vartheta)}{x}\right|_{x(\vartheta)}$$

to illustrate the complicated relationship between parameters and linearized dynamics. The tangent manifold of a scalar system such as Eqn. (7.1) may be parameterized in ϑ in two steps,

$d(x)$	Convexity	$\frac{\partial^2}{\partial \vartheta^2} A(\vartheta)$
$x^3 + c_1 x^2 + c_2 x$	In general no	see Fig. 7.1
$\sin x$	Locally Convex	$\left(1-\vartheta^2\right)^{-\frac{3}{2}}$, $-1 < \vartheta < 1$
$\log x$	Concave	$-e^{-\vartheta}$

Table 7.1: Nonconvexity of nonlinear dynamics $d(x)$

1. *Solve* $f(x, \vartheta) = 0$ *for* $x(\vartheta)$

2. *Compute* $A(x, \vartheta) = \dfrac{\partial f(x, \vartheta)}{x}$ *and substitute* $x(\vartheta)$ *from Step 1 to obtain* $A(\vartheta)$

The convexity of $A(\vartheta)$ *for three nonlinear functions* $d(x)$ *are computed in Table 7.1. In general, if the linearized system is convex in* ϑ*, it is locally convex and depends on* ϑ*. This is the case for a polynomial and sinusoidal* $d(x)$*. For the case of* $d(x) = \log x$*, global concavity is independent of* ϑ*. Also note that local stability is a function of* ϑ*. For each nonlinear function* $d(x)$*, Table 7.1 summarizes the convexity result and computes the second derivative test of convexity for* $A(\vartheta)$*.*

Figure 7.1 illustrates the complicated relationship between parameters and linearized dynamics for a polynomial case

$$d(x) = x^3 - 3x$$

The leftmost subplot Fig. 7.1(a) shows $d(x)$*. For this example ,* $x(\vartheta)$ *from Step 1 can be found by rotating the plot* 90° *clockwise as shown in Fig. 7.1(b). The result of Step 2. above is shown in 7.1(c). Clearly* $A(\vartheta)$ *is not convex in* ϑ*; in fact, it is not even a well defined function of* ϑ*.*

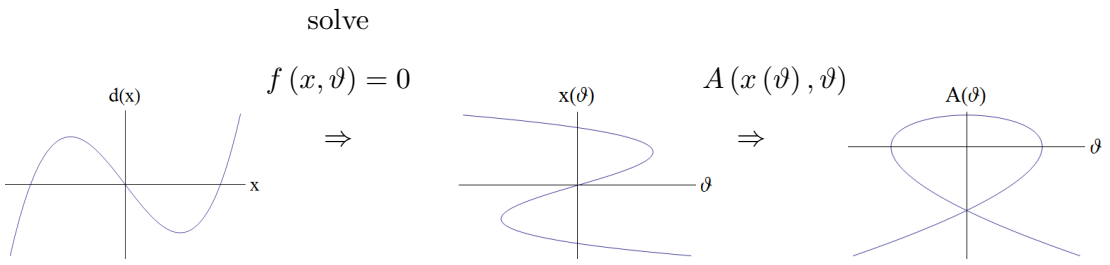

Figure 7.1: Parameter dependent dynamics for polynomial $d(x)$: from left to right (a) $d(x)$ vs. x; (b) $x(\vartheta)$ vs. x; (c) $A(\vartheta)$ vs. ϑ

Also note that local stability is a function of ϑ and is not related to convexity. All of the above systems may be stable, e.g. $-x^3$ is globally stable, $-\sin x$ is locally stable, and $-\log x$ is stable where it is defined.

The preceding example shows that the convex polytopes used to simplify and solve the MMAR covering problem in Sec. 4.3 will not in general apply to families of plants generated from nonlinear systems. Unfortunately the loss of convexity complicates controller covering and computation. This loss of convexity in the family of linearized plants motivates future work on control covering and Lyapunov switch logic applied directly to the nonlinear plant.

A grid may be applied to the parameter space and local convexity conveys to grid tiles. The grid must be sufficiently dense to capture variation in $\Gamma(\vartheta)$. This block LMI computation uses a possibly large set of grid vertices $\{\vartheta_{ij}\}$. A grid is used to compute a family of plants in Sec. 7.2 below.

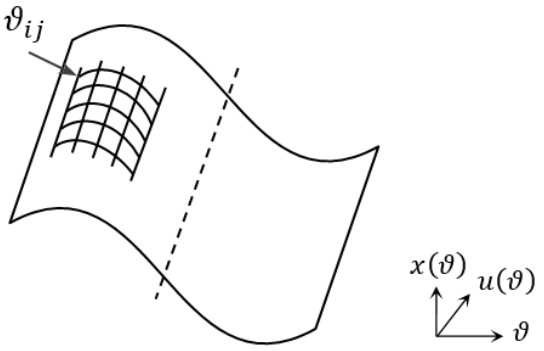

Figure 7.2: Plant Set Vertices $\{\vartheta_{ij}\}$ on Equilibrium Surface of a Nonlinear System

Careful choice of coordinates for the equilibrium surface of the nonlinear system may facilitate grid and controller design. Refer to Fig. 5.3 and observe that the equilibrium surface is multivalued in coordinate κ due to the top and bottom sheets. In general the parameters ϑ may fail to uniquely define the manifold $\mathcal{E}^*$. Computing a global parametric representation of an implicit manifold is a difficult problem. The zero structure deficiencies described in Sec. 2.3 further complicate these computations. The independent variables used to compute the equilibrium surface are the parameters (v^*, κ), but other coordinate choices are available. Two categories for parameterizing the manifold $\mathcal{E}^*$ are considered

1. An atlas with two charts:

   (a) For this example the coordinates (v^*, κ, σ^*) where $\sigma^* \in \{B, T\}$ are sufficient. Here B, T enumerate the Bottom and Top equilibrium sheets respectively.

   (b) The coordinate set $(v^*, \alpha^*, \sigma^*)$ would be a similar choice but with a measurable state (α). The use of measurable coordinates combined with fore knowledge of the equilibrium surface may facilitate final state (x_f) computation.

2. Local parameterization: The equilibrium surface may be locally parameterized as a composition of flows of the span of the null space as suggested in [KC98]. In this case, the equilibrium surface is parameterized by coordinates s_1, s_2. See Example 7.2

below. This injective parameterization may be superior for control design near the singular surface.

Example 7.2. *Compare the equilibrium surfaces derived by the local parameterization of [KC98] with a pointwise computed grid. Compute the null space of the longitudinal dynamics Eqn. (5.1). The ProPac function* ExpMap *is convenient for computing the local flows of a vector field spanning the null space. The ProPac function* FlowComposition *composes the integral curve. The equilibrium surface requires two coordinates* s_1, s_2 *and the origin* $[s_1\, s_2] = 0$ *is chosen to be the singular surface point along the velocity slice* $v = 0.6$. *The coordinates* s_1,s_2 *map to variables* $v, \kappa, \alpha, \delta$ *as follows:*

$$
\begin{aligned}
v(s_1, s_2) &\approx 0.38s_1^3 - 5.4s_1^2 s_2 + 0.6s_1^2 - 13s_1 s_2^2 + 1.3s_1 s_2 - 0.01s_1 - 80s_2^3 + 13s_2^2 - 2.2s_2 + 0.6 \\
\kappa(s_1, s_2) &\approx -1.1s_1^3 + 6.8s_1^2 s_2 - 1.7s_1^2 + 18.0s_1 s_2^2 - 3.6s_1 s_2 + 0.02s_1 - 49s_2^3 + 6.2s_2^2 - 1.0s_2 + 0.15 \\
\alpha(s_1, s_2) &\approx 0.12 + s_2 \\
\delta(s_1, s_2) &\approx 0.25 + s_1
\end{aligned}
$$

Figure 7.3 compares this locally derived, parameterized equilibrium surface with the surface of Fig. 5.3. The green and red shaded sections are the Bottom and Top equilibrium sheets from Fig. 5.3. The s_1 *and* s_2 *axes are the black horizontal lines and the red vertical lines respectively. The origin* $(s_1, s_2) = 0$ *is the intersection of the thick black and red lines. Observe from Fig. 7.3 that the equilibrium surface derived here is an accurate approximation of the surface in Fig. 5.3.*

Remark 7.3. *In the case of multiple equilibrium sheets, two or more sheets may have similar zero structure such that regions on these disjoint sheets share common quadratic stability. A parameterization different from the above may be desired. This parameterization arranges the tangent bundle subspace* Γ_ϑ *according to common quadratic stability. The mapping from parameter space* ϑ *to the elements of* $\{A(\vartheta), B(\vartheta), C(\vartheta)\}$ *of Eqn. (5.5) would be onto but not one-to-one. For this shared stability case a simple equivalence test for common quadratic stability would be helpful but such a test is an open problem.*

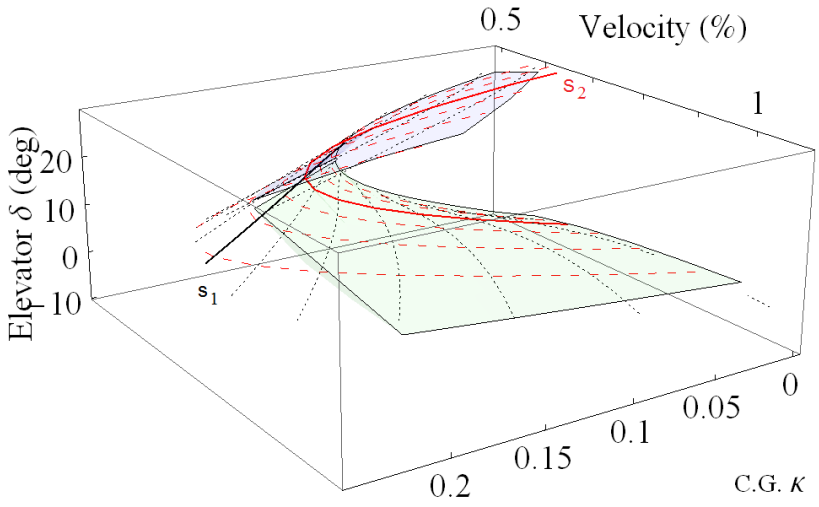

Figure 7.3: Equilibrium surface from local parameterization and pointwise computations

Now apply the linearization process of Sec. 5.2.1 on the pointwise computed equilibrium surface shown in Fig. 5.3 and Fig. 7.3 to obtain a family of plants for controller design.

7.2 Parameter Dependent Family of Plants

The process of Sec. 5.2.1 is used to obtain a linear family of plants from the equilibrium surface of the nonlinear dynamics. The equilibrium constraint $\mathcal{E} = 0$ for system Eqn. (5.1) is $n + p = 6$ equations in $n + m + k = 9$ variables with $k = 3$ parameters: (v^*, γ^*, κ). This example considers only level flight $(\gamma^* = 0)$ such that $k = 2$ and the equilibrium surface is 2-D as shown in Sec. 5.3.2 and Fig. 5.3.

Evaluate the linearization equations along the equilibrium surface $\mathcal{E}^*$ to obtain a finite set of approximately 150 plants for regulator design. This finite set is a subset of the continuous family $\mathcal{P}$ as represented by the shaded regions of the equilibrium surface in Fig. 5.3. The finite subset excludes $\mathbf{p}(\vartheta) \in \mathcal{P}$ near the singular surface where for this example controllability is lost.

As an example of the family $\mathcal{P}$ consider plants taken from the two equilibrium branches of Fig. 5.2. The plants are taken from the bottom and top equilibrium branches as shown

Surface	$A(\vartheta)$	$B(\vartheta)$
Bottom	$\begin{bmatrix} -0.73 & -0.67 & -1 & 0 \\ -7.7 & -10.1 & 0 & 1 \\ 0 & 0 & 0 & 1 \\ 0 & -64.3 & 0 & -8 \end{bmatrix}$	$\begin{bmatrix} 0.98 & 0.03 \\ -0.38 & -0.92 \\ 0 & 0 \\ 0 & -126.5 \end{bmatrix}$
Top	$\begin{bmatrix} -0.64 & -0.89 & -1 & 0 \\ -7.8 & -7.9 & 0 & 1 \\ 0 & 0 & 0 & 1 \\ 0 & 232.7 & 0 & -8 \end{bmatrix}$	$\begin{bmatrix} 0.98 & -0.19 \\ -0.38 & 1.3 \\ 0 & 0 \\ 0 & 170.5 \end{bmatrix}$

Table 7.2: Linearized Plant Matrices ($\kappa = 0.05$) for Aero Example

by "B" and "T" along the line $\kappa = 0.05$ in Fig. 5.2 (where $v^* = 0.5$). The linearized plant from the bottom branch shown in Row 1 of Table 7.2 is located inside the region of open loop stability. The linearized plant from the top branch shown in Row 2 of Table 7.2 has a zero structure different from the bottom branch sub-family of plants and is open loop unstable.

The set-points v^*, γ^* are mapped to the outputs with a binary matrix F as follows,

$$F = - \begin{bmatrix} 1 & 0 \\ 0 & 1 \end{bmatrix}$$

The matrix E can be used to translate the origin by computing

$$E\vartheta = - (Ax + Bu)$$

where u is Kx. For convenience ϑ can be fixed to 1 and the elements of F adjusted to the set-points.

7.3 Regulator Design

The following two sections obtain the $\{P_i\}$ for switch logic and the $\{K_i\}$ for control covering.

7.3.1 Common Quadratic Lyapunov Function

A CQLF matrix P_i which satisfies Eqn. (4.8) is obtained by simultaneously solving sets of inequalities (4.2) in the block LMI of Eqn. (4.5) as detailed in Sec. 4.2. The composite design matrices of Sec. 4.4.1 are

$$A_j = \begin{bmatrix} A(\vartheta) & 0 \\ JC & Z \end{bmatrix}, B_j = \begin{bmatrix} B(\vartheta) \\ 0 \end{bmatrix}$$

and are uniquely defined by coordinates $\vartheta = (v^*, \kappa, \sigma)$. The parameter dependent matrices $A(\vartheta)$ and $B(\vartheta)$ were obtained in the preceding section. The C matrix is independent of ϑ in this example and thus identical for all $\mathbf{p}(\vartheta) \in \mathcal{P}$. The regulated outputs are $\begin{bmatrix} v & \gamma \end{bmatrix}^T = Cx$ such that

$$C = \begin{bmatrix} 1 & 0 & 0 & 0 \\ 0 & -1 & 1 & 0 \end{bmatrix}$$

The regulator design matrices for the internal model Z and error update gains J are $J = I_2$, $Z = 0_2$.

The composite plant plus controller state vector $\bar{x}$ is dimension $n + p = 6$,

$$\bar{x} = [v,\ \alpha,\ \theta,\ q,\ \eta_1,\ \eta_2]^T$$

The LQR design weights of (4.1) have form

$$\begin{bmatrix} C_z & D_z \end{bmatrix} = \begin{bmatrix} Q_z & 0 \\ 0 & R_z \end{bmatrix}$$

where for both subfamilies $Q_z = I_{n+p}$, $R_z = I_p$.

The composite design matrices A_j, B_j and design weights C_z, D_z are used in Eqn. (4.2) to form approximately 100 and 50 inequalities for the bottom and top surface respectively. These inequalities are concatenated into LMIs of form Eqn. (4.5) and solved for a CQLF. A single CQLF was obtained for each of the top and bottom equilibrium surface regions seen as shaded portions of Fig. 5.3. Since controllability is lost at the singular surface the unshaded portions of Fig. 5.3 are not guaranteed stable by the CQLFs. Given the above design weights the CQLF for the top equilibrium sheet is

7.3.2 State Feedback Controller

Recall that a single matrix $B_i \in Co\{B(\vartheta_{ij})\}$ is used to form the LQR state feedback gain $K_i = -\left(D_z^T D_z\right)^{-1} B_i^T P_i$ for the region Ω_i. In general choose B_i such that $\|K\|_2$ is minimized to improve robustness to unmodeled error. In this example the matrix $B(\vartheta_{ij})$ that minimizes $\|B(\vartheta)\|_2$ over $\vartheta \in \Omega_i$ was chosen as B_i. This selection of B_i for Eqn. (4.6) per Eqn. (4.7) such that Eqn. (4.8) holds is detailed in Table 7.4.

The state feedback K_B and K_T of Eqn. (2.7) are given in Table 7.3.

The previous Sec. 7.3.1 solves inequalities Eqn. (4.2) simultaneously in the block form of Eqn. (4.5) for a P_i. However, if upon selection of B_i, Eqns. (4.8) do not hold with this P_i, then with inputs B_i and K_i simultaneously solve inequalities Eqns. (4.8) in block form to alter P_i for use in switch logic Eqn. (3.5). For the choices of B_i, $i \in \{B, T\}$, in Table 7.4, only P_B must be altered by solving Eqns. (4.8).

7.4 Simulation

In case of an unanticipated change in the aircraft longitudinal dynamics, the "true" longitudinal dynamics may be imprecisely known. As shown in Sec. 2.3, a single regulator may fail to simultaneously regulate the aircraft due to zero structure change. The two locations on the equilibrium curve listed in Table 7.2 and pictured in Fig. 5.2 are simulated.

	Equilibrium Sheet	
	Bottom	Top
P_i	$\begin{bmatrix} 1.8 & 0.11 & -1.4 & -0.02 & 2.4 & -0.09 \\ 0.11 & 0.8 & -0.16 & 0.02 & 0.17 & -0.06 \\ -1.4 & -0.16 & 2. & 0.06 & -2.6 & 0.31 \\ -0.02 & 0.02 & 0.06 & 0.03 & -0.01 & 0.04 \\ 2.4 & 0.17 & -2.6 & -0.01 & 5.2 & 0.1 \\ -0.09 & -0.06 & 0.31 & 0.04 & 0.1 & 0.29 \end{bmatrix}$	$\begin{bmatrix} 3.9 & -1.6 & -0.16 & -0.06 & 0.96 & 0.5 \\ -1.6 & 4.8 & 0.29 & 0.29 & -0.12 & -0.02 \\ -0.16 & 0.29 & 2.4 & 0.08 & -0.91 & 1.2 \\ -0.06 & 0.29 & 0.08 & 0.04 & -0.03 & 0.03 \\ 0.96 & -0.12 & -0.91 & -0.03 & 5.5 & -0.22 \\ 0.5 & -0.02 & 1.2 & 0.03 & -0.22 & 2.1 \end{bmatrix}$
K_i	$\begin{bmatrix} -2.2 & 0.24 & 0.16 & 0.01 & -0.91 & -0.77 \\ -0.4 & 0.79 & 2.4 & 1. & -0.73 & 1.3 \end{bmatrix}$	$\begin{bmatrix} -4.1 & 2.5 & 0.22 & 0.12 & -0.98 & -0.5 \\ 1.8 & -9.8 & -2.5 & -1.2 & 0.96 & -1.2 \end{bmatrix}$

Table 7.3: Lyapunov matrix (P_i) and LQR gain (K_i) for the MIMO Example

Sheet	Region	ϑ coordinates (v^*, κ, σ^*)	$\|K\|_2$
Bottom	Ω_B	$\vartheta_{ij} = (0.5, 0.1, B)$	3.20
Top	Ω_T	$\vartheta_{ij} = (0.6, 0.15, T)$	10.97

Table 7.4: Selection of B_i to minimize $\|K\|_2$

The aircraft is nominally trimmed to the open loop stable "Bottom" plant when an event occurs at $t = 1$ sec. The "true" plant for $t \geq 1$ is then the "Top" plant. The zero structure and coordinate σ changes. Just two state feedback controllers are sufficient to regulate all plants in $\mathcal{P}$.

Details of the plant and controller simulation components can be found in the following subsections:

1. Plant Family $\mathcal{P}$: Section 7.2, Table 7.2
2. Control Gains K_i: Section 7.3.2
3. Switch Logic: Section 3.2
4. CQLF P_i: Section 7.3.1

These four components are assembled into the MMAC structure of Fig. 1.2.

The MMAC is simulated in Mathematica. A numerical solution to the set of first order differential equations is obtained with *NDSolve* with a fixed step solver at 1kHz. The discrete state is accommodated by adding *WhenEvent* logic to *NDSolve*. The Lyapunov switch logic inequality is evaluated at 1kHz. Sample code is included in Appendix B.

Initial conditions for the plant (x), controller (η), exogenous disturbance (ϑ), switch logic index (σ) states and parameters (v^*, κ, σ) are specified as follows

Time	Plant Equil. Sheet (v^*, κ, σ^*)	Lyapunov Metric $\left(\dot{V}_i\right)$	Switch Logic State $(\sigma(t))$
$t < 1$	$(0.5, 0.05, B)$	$\dot{V}_B < 0$	$\sigma \to B$
$t = 1$	plant dynamics change		
$t > 1$	$(0.5, 0.05, T)$	$\dot{V}_T < 0$	$\sigma \to T$

Table 7.5: Simulation Timeline

$$
\begin{aligned}
\left[v(0)\ \alpha(0)\ \theta(0)\ q(0) \right] &= \begin{bmatrix} 1.1v^* & \alpha^* & 1.1\theta^* & q^* \end{bmatrix} \\
\begin{bmatrix} \eta_1(0) & \eta_2(0) \end{bmatrix} &= \begin{bmatrix} 0 & 0 \end{bmatrix} \\
\begin{bmatrix} \vartheta_1(0) & \vartheta_2(0) \end{bmatrix} &= \begin{bmatrix} v^* & 0 \end{bmatrix} \\
\sigma(0) &= B \\
(v^*, \kappa) &= (0.5, 0.05) \\
\sigma^* &= \begin{cases} B & t < 1 \\ T & t \geq 1 \end{cases}
\end{aligned}
$$

The simulation timeline is shown in Table 7.5.

The final value of the composite state is defined as

$$
\bar{x}^*(v^*, \kappa, \sigma^*) \equiv \begin{bmatrix} v^* & \alpha^* & \theta^* & q^* & \eta_1^* & \eta_2^* \end{bmatrix}
$$

where $q^* = 0$ and $\theta^* - \alpha^* = \gamma^*$. The controller states (η_1^*, η_2^*) are zero if the parameter values are equilibrium values. In other words, if (v^*, γ^*, κ) are consistent with an equilibrium point $\mathcal{E}(x^*, u^*, \vartheta^*) = 0$, then $\eta_i^* = 0$. For $t \geq 1$ the final state is

$$\bar{x}^*\left(0.5, 0.05, T\right) = \left[\begin{array}{cccccc} 0.5 & 0.116 & 0.116 & 0 & 0 & 0 \end{array}\right]$$

The bounded Lyapunov functions V_i, $i \in \{B, T\}$, of Fig. 7.6 show internal stability. The Lyapunov functions are normalized such that $V\left(0\right) = 100\%$. The time rate of change of the Lyapunov functions V_i, $i = \{B, T\}$ are shown in Fig. 7.5. The switch logic quickly responds $\left(< \frac{1}{100} \text{ secs}\right)$ as seen in Fig. 7.4(a). Thus K_B regulates toward an equilibrium on the "Bottom" sheet for $t < 1$ and then the correct controller, K_T is quickly switched on for $t > 1$. Successful output regulation $\lim_{t\to\infty} e\left(t\right) = 0$ is shown in Fig. 7.4(b).

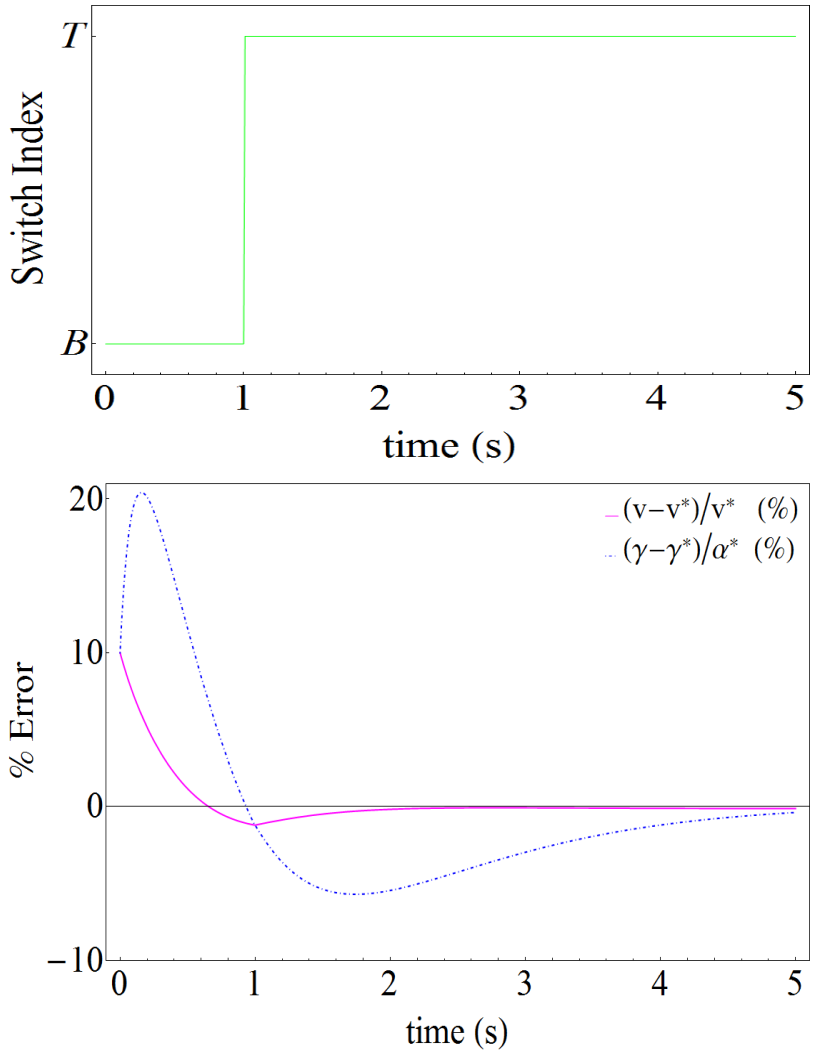

Figure 7.4: MMAR Aero Simulation: (a) Switch Index σ (above); (b) Regulation Error e

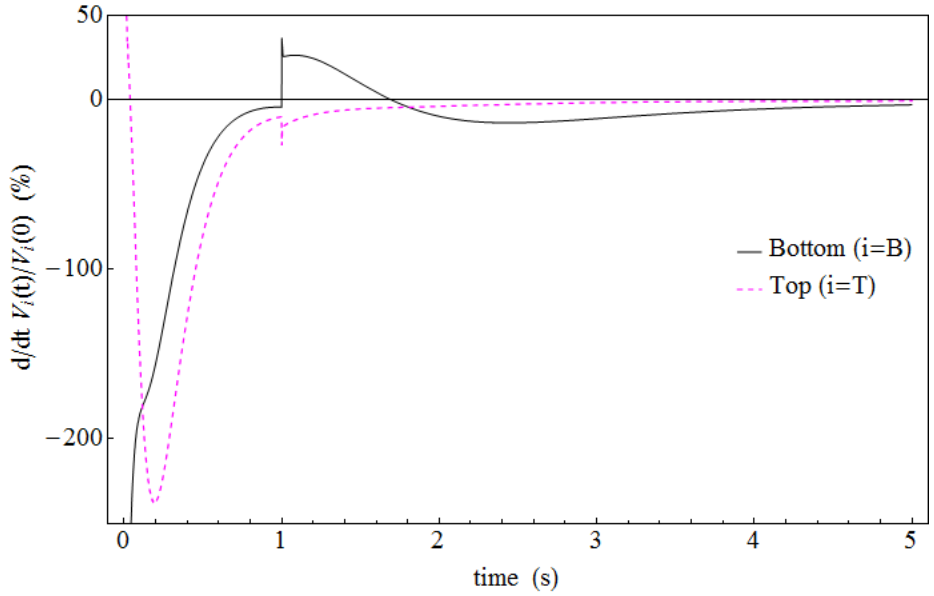

Figure 7.5: MMAR Aero Simulation Normalized Lyapunov Rate: $\frac{d}{dt}V_i(t)/V_i(0)$ (%)

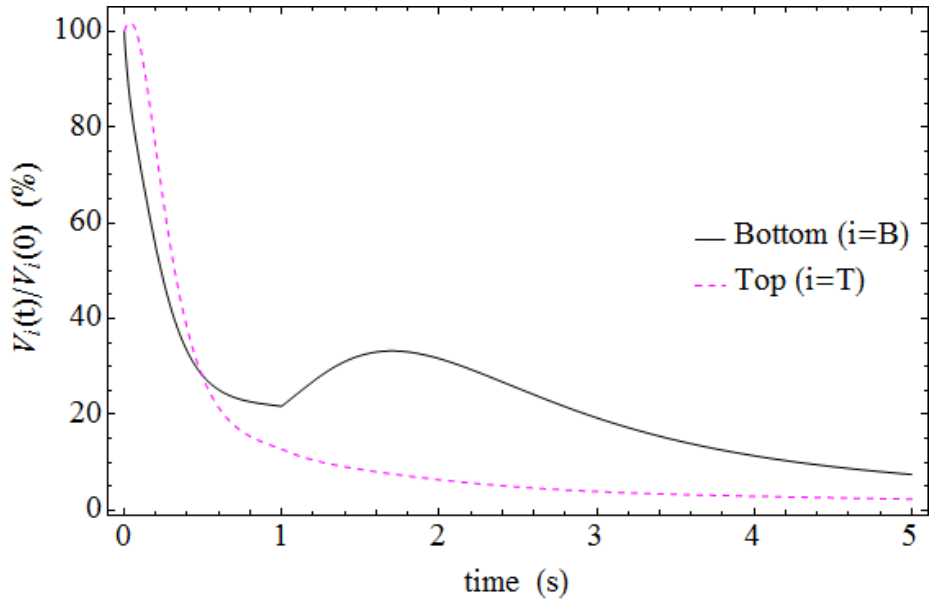

Figure 7.6: MMAR Aero Simulation Normalized Lyapunov Function: $V_i(t)/V_i(0)$ (%)

8. CONCLUSION

8.1 Summary

The hybrid system developed in this thesis uses discrete states with switch logic along with continuous controllers to improve system safety. A multiple model controller that combines a Linear Quadratic Regulator (LQR) state feedback design and Common Quadratic Lyapunov Function (CQLF) is introduced. The design procedure has been detailed. Specifically the choice of plants in the parameter space and the selection of the design matrices are detailed and proven. This multiple model adaptive regulator is implemented on parameter dependent systems with diverse zero structure.

It is well known that regulation is not possible at points of zero structure change. Less well known is that regulation by a common controller is not possible across points of zero structure change. Thus, a common controller can only be used as parameters vary within a family having equivalent zero structure. A finite set of controllers with switch logic enables robust adaptive regulation.

In general, a multiple model controller design presents two subproblems, control covering and switching. The control covering subproblem is solved with a familiar LQR state feedback design. The switching subproblem is solved with Lyapunov function based switch logic. The multi-model design subproblems are both quadratic and convex. Hence both subproblems may be solved concurrently as a set of linear matrix inequalities. The design is suitable for complex systems since fast, accurate solutions of large LMIs are possible. This is a significant improvement over previous trial and error approaches to control covering and switch logic design.

In addition to unified computation, the controller covering of the parameter space has been simplified. Previous MMAC designs exploit controller robustness properties to cover the parameter space. These robustness properties may lack simple geometric interpretations

in the parameter space. In contrast, the design proposed in this thesis exploits the convexity of the LMI to cover the parameter space with simple, convex polytopes like triangles and rectangles. These shapes accommodate the abrupt changes in simultaneous regulation of systems with diverse zero structure.

The unified approach to control and switch logic design prompted specific implementation questions. A result on the flexibility in the choice of the state feedback gain is proved in Section 4.3.1. A limitation to the type of regulator design in also shown. Lastly, methods to mitigate the Lyapunov function dependence on a priori knowledge of the final state are provided. Thesis contributions are detailed in Section 1.4.2.

The multiple model adaptive regulator is implemented on a linear system with linear dependence in the unknown parameter in Chapter 6. Since the system matrix and hence zero structure are linear in the parameters, the set of plants with equivalent zero structure are linear, and hence convex, in the parameters. The convex set of parameter dependent plants coupled with the convexity of the LMI allows for a geometrically appealing control covering.

The multiple model adaptive regulator is implemented on a linear family of plants derived from the linearization of a nonlinear, longitudinal aircraft dynamics model in Chapter 7. In general, the system matrix of the parameter dependent linearized family of plants is not linear in the parameters and hence a convex covering of the parameter space is not possible. For the longitudinal aircraft dynamics model, two controllers are sufficient for regulation in a neighborhood of the equilibrium surface over a large portion of the flight envelope. Simulation results are provided.

8.2 Future Research

As with many experiments, more questions are uncovered than answered. Recommendations for future research are summarized below.

Final State Information The major benefit of robust regulation is insensitivity to both parameter variation and external disturbances. The insensitivity to parameter variation adds robustness to our MMAR design. The insensitivity to external disturbances effects a translation of the final state. And this translation complicates the Lyapunov function switch logic since Lyapunov logic requires precise knowledge of the final state. Two methods to circumvent this lack of a priori knowledge of the final state are presented in Section 3.2.2, but these methods may be too slow. If an erroneous controller is allowed to persist in closed loop the system may exit the region of safe operation. Moreover, if the set of possible controllers is large, time spent evaluating individual controllers can create large delays such that the system may exit the region of safe operation.

Switch Logic This paper implements a prerouted, trial and error switch logic. As mentioned in Sec. 1.3 and references [AM02] & [MA01], other forms of switch logic have been studied. The approach implemented here is sufficient for a small set of controllers. But a larger set of controllers may require a more intelligent winnowing of the set of possible controllers before testing a controller "in the loop." The question is then how to infer the proper controller? In addition, what can be learned from previous, incorrect controllers? The multiple model approach adds a unique form of persistent excitation.

Implementation questions regarding the robustness of the switch logic to noise, modeling error, and final state uncertainty have not been quantified. For example, a design trade-off between switch speed and robustness is anticipated.

Strict Equivalence Note that only a change in the "equivalent" zero structure across a singular surface has been defined. A comprehensive definition of zero structure equivalence has not been developed. The definition of strict equivalence in [GS00] for example is more restrictive than our implied definition. As defined in [GS00], strict equivalent matrices have the same finite & infinite divisors and row & column indices. Note that the finite divisors are the same only if the transmission zeros have equivalent numerical values. For our purposes

the zero "structure" is more important than individual values of the transmission zeros.

Common Quadratic Lyapunov Functions As mentioned in Remark 7.3, a simple test for the existence of a CQLF for two matrices is an open question. An existence test would facilitate the control covering. Necessary and sufficient tests for the existence of a CQLF have been identified for the 2×2 matrix case. These existence tests may use the eigenvalues of the product of two matrices, products involving inverses, or convex combinations of these. But results for higher dimensions remain elusive. For this problem, a characterization of the existence of a CQLF for parameter dependent matrices would be helpful. In the absence of such a characterization, a trial and error method using convex, numeric LMI solvers is the only reliable existence test. In addition, the use of non-quadratic level sets has not been explored.

Bibliography

[ABDB+00] Brian DO Anderson, Thomas S Brinsmead, Franky De Bruyne, Joao Hespanha, Daniel Liberzon, and A Stephen Morse. Multiple model adaptive control. part 1: Finite controller coverings. *International Journal of Robust and Nonlinear Control*, 10(11-12):909–929, 2000.

[ACD+77] Michael Athans, David Castanon, K-P Dunn, C Greene, Wing Lee, N Sandell Jr, and Alan S Willsky. The stochastic control of the f-8c aircraft using a multiple model adaptive control (mmac) method–part i: Equilibrium flight. *IEEE Transactions on Automatic Control*, 22(5):768–780, 1977.

[AM02] D. Angeli and E. Mosca. Lyapunov-based switching supervisory control of nonlinear uncertain systems. *IEEE Transactions on Automatic Control*, 47(3):500–505, 2002.

[BEFB94] S. Boyd, L. El Ghaoui, E. Feron, and V. Balakrishnan. *Linear Matrix Inequalities in System and Control Theory*. SIAM, Philadelphia, PA, 1994.

[Ber93] Jordan M Berg. *Unfolding of singular pencils with applications to control systems*. PhD thesis, Drexel University, 1993.

[BFS88] B Ross Barmish, Minyue Fu, and S Saleh. Stability of a polytope of matrices: Counterexamples. *IEEE Transactions on Automatic Control*, 33(6):569–572, 1988.

[BG02] Bassam Bamieh and Laura Giarre. Identification of linear parameter varying models. *International Journal of Robust and Nonlinear Control*, 12(9):841–853, 2002.

[BK94] J. Berg and H. G. Kwatny. An upper bound on the structurally stable regulation of a parameterized family of nonlinear control systems. *Systems and Control Letters*, 23:85–95, 1994.

[Bos08] J. D. Boskovic. An integrated approach to damage accommodation in flight control. In *AIAA Guidance, Navigation, & Control Conference*, Honolulu, HI, August 2008.

[Che84] C.T. Chen. *Linear System Theory and Design*. Oxford series in electrical and computer engineering. Oxford University Press, 1984.

[Dav72] E. J. Davison. The output control of linear time-invariant multivariable systems with unmeasurable arbitrary disturbances. *IEEE Transactions on Automatic Control*, AC-17(5):621–630, 1972.

[DG08] Guillaume Ducard and Hans P. Geering. Efficient nonlinear actuator fault detection and isolation system for unmanned aerial vehicles. *Journal of Guidance, Control, and Dynamics*, 31(1):225–237, 2008.

[FB86] Minyue Fu and B. Ross Barmish. Adaptive stabilization of linear systems via switching control. *IEEE Transactions on Automatic Control*, 31(12):1097–1103, 1986.

[Fra77] B. A. Francis. The linear multivariable regulator problem. *SIAM Journal on Control and Optimization*, 15:486–505, 1977.

[FW75a] B. A. Francis and W. M. Wonham. The internal model principle for linear multivariable regulators. *Applied mathematics and optimization*, 2(2):170–194, 1975.

[FW75b] Bruce A Francis and William M Wonham. The role of transmission zeros in linear multivariable regulators. *International Journal of Control*, 22(5):657–681, 1975.

[GS00] F.R. Gantmakher and American Mathematical Society. *The Theory of Matrices*. Number v. 2 in AMS Chelsea Publishing Series. American Mathematical Society, 2000.

[HLM03] Joao P Hespanha, Daniel Liberzon, and A Stephen Morse. Overcoming the limitations of adaptive control by means of logic-based switching. *Systems & Control Letters*, 49(1):49–65, 2003.

[HLSM+01] Joao Hespanha, Daniel Liberzon, A Stephen Morse, Brian Anderson, Thomas S Brinsmead, and Franky De Bruyne. Multiple model adaptive control. part 2: switching. *International journal of robust and nonlinear control*, 11(5):479–496, 2001.

[HM99] Joao P Hespanha and A Stephen Morse. Stability of switched systems with average dwell-time. In *Decision and Control, 1999. Proceedings of the 38th IEEE Conference on*, volume 3, pages 2655–2660. IEEE, 1999.

[Isi95] A. Isidori. *Nonlinear Control Systems*. Springer-Verlag, London, 3 edition, 1995.

[KB00] H. G. Kwatny and G. L. Blankenship. *Nonlinear Control and Analytical Mechanics: a computational approach*. Control Engineering. Birkhauser, Boston, 2000.

[KBB91] H. G. Kwatny, W. H. Bennett, and J. M. Berg. Regulation of relaxed stability aircraft. *IEEE Transactions on Automatic Control*, AC-36(11):1325–1323, 1991.

[KC98] H. G. Kwatny and B. C. Chang. Constructing linear families from parameter-dependent nonlinear dynamics. *IEEE Transactions on Automatic Control*, 43(8):1143–1147, 1998.

[Kha02] H.K. Khalil. *Nonlinear Systems*. Prentice Hall, New Jersey, 2002.

[KK78] H. G. Kwatny and K. C. Kalnitsky. On alternative methodologies for the design of robust linear multivariable regulators. *IEEE Transactions on Automatic Control*, AC-23(5):930–933, 1978.

[KS72] H. Kwakernaak and R. Sivan. *Linear optimal control systems*. Wiley-Interscience New York, 1972.

[Löf04] J. Löfberg. Yalmip : A toolbox for modeling and optimization in matlab. In *IEEE Int. Sym. on Computer Aided Control Systems Design*, pages 284–289, Sept. 2004.

[MA01] Edoardo Mosca and Tommaso Agnoloni. Inference of candidate loop performance and data filtering for switching supervisory control. *Automatica*, 37(4):527–534, 2001.

[Mår85] Bengt Mårtensson. The order of any stabilizing regulator is sufficient a priori information for adaptive stabilization. *Systems & Control Letters*, 6(2):87–91, 1985.

[MD89] Daniel E Miller and EJ Davison. An adaptive controller which provides lyapunov stability. *IEEE Transactions on Automatic Control*, 34(6):599–609, 1989.

[MGHM88] Richard H Middleton, Graham C Goodwin, David J Hill, and David Q Mayne. Design issues in adaptive control. *IEEE Transactions on Automatic Control*, 33(1):50–58, 1988.

[MMG92] A Stephen Morse, David Q Mayne, and Graham C Goodwin. Applications of hysteresis switching in parameter adaptive control. *IEEE Transactions on Automatic Control*, 37(9):1343–1354, 1992.

[Mor90] AS Morse. Towards a unified theory of parameter adaptive control: tunability. *IEEE Transactions on Automatic Control*, 35(9):1002–1012, 1990.

[Mor96] A Stephen Morse. Supervisory control of families of linear set-point controllers part i. exact matching. *IEEE Transactions on Automatic Control*, 41(10):1413–1431, 1996.

[MP89] Peter S Maybeck and Donald L Pogoda. Multiple model adaptive controller for the stol f-15 with sensor/actuator failures. In *Decision and Control, 1989., Proceedings of the 28th IEEE Conference on*, pages 1566–1572. IEEE, 1989.

[NB94] Kumpati S Narendra and Jeyendran Balakrishnan. Improving transient response of adaptive control systems using multiple models and switching. *IEEE Transactions on Automatic Control*, 39(9):1861–1866, 1994.

[NB97] K. S. Narendra and J Balakrishnan. Adaptive control using multiple models. *IEEE Transactions on Automatic Control*, 42(2):171 – 187, February 1997.

[PBKG08] T Zajic Prasanth, J Boškovic, N Knoebel, and I Gregory. Model set reduction with application to damage adaptive flight control. In *Proceedings of the 2008 AIAA Guidance, Navigation & Control Conference, Honolulu, Hawaii*, pages 18–21, 2008.

[PK01] Felipe M Pait and Fuad Kassab. On a class of switched, robustly stable, adaptive systems. *International Journal of Adaptive Control and Signal Processing*, 15(3):213–238, 2001.

[PK14] E. Peterson and H. Kwatny. Multi-model adaptive regulation for a family of systems containing different zero structures. In *IFAC World Congress*, volume 19, page To Appear, 2014.

[PKT+94] Kameshwar Poolla, Pramod Khargonekar, Ashok Tikku, James Krause, and Krishan Nagpal. A time-domain approach to model validation. *IEEE Transactions on Automatic Control*, 39(5):951–959, 1994.

[Sal12] Mishah Uzziél Salman. *Control of aircraft operating under adverse conditions*. PhD thesis, 2012.

[SL91] Jean-Jacques E Slotine and Weiping Li. *Applied nonlinear control*. Prentice-Hall Englewood Cliffs, NJ, 1991.

[VODM96] Peter Van Overschee and B De Moor. Subspace identification for linear systems: Theory, implementation, applications. *Kluwer Academic Publishers*, 1996.

[ZDG+96] Kemin Zhou, John Comstock Doyle, Keith Glover, et al. *Robust and optimal control*, volume 40. Prentice Hall New Jersey, 1996.

Appendix A. ABBREVIATIONS AND SYMBOLS

Acronyms

LQR	Linear Quadratic Regulator
LMI	Linear Matrix Inequality
MMAC/MMAR	Multiple Model Adaptive Control/Regulator
SISO	Single Input Single Output
MIMO	Multi Input Multi Output
CQLF	Common Quadratic Lyapunov Function
ARE	Algebraic Riccati Equation

General Notation

$\mathbf{p}(\theta)$	Family of Parameter Dependent Linear Plants
P_i, $\mathcal{P}$	Plant, Family of Plants
C_i, $\mathcal{C}$	Controller, Set of Controllers
$V(t)$	Lyapunov Function
$\sigma(M)$	Spectrum of matrix M
λ	eigenvalue
s	Laplace Variable
δ_v	v-gap Metric
Ω	Region of parameter space
θ_{ij}	j'th vertex of region Ω_i
θ_{k}	k'th element of parameter vector
$\mathbb{C}$, $(\mathbb{C}^-)$	Complex Plane, (left half with negative real part)
$\mathcal{E}^*$	Equilibrium Surface
$\ker M$	kernel of matrix M (i.e. null space)
$\mathrm{im}M$	image of matrix M

Longitudinal Aerodynamics Example

v, α, θ, q	Longitudinal Aircraft states: velocity, angle of attack, pitch, pitch rate
Π, δ	Thrust and elevator inputs
γ	Flight Path Angle
κ	Center of gravity parameter

Control System Notation

$f(\cdot)$	state dynamics
x	Plant state vector
$\dot{x}$	$\frac{d}{dt}x$
u	System Input
θ	Parameters
ϑ	Exogenous system states
A, B, C, D	Plant Matrices
E, F	Disturbance Input Matrices
P_i	Lyapunov Function Matrix
K_i	State Feedback Gain
Z	Exogenous System /Internal Model Dynamics
Γ	System Matrix
x_c	Compensator state vector
$\bar{x}$	Composite plant & compensator state vector (i.e. $[x\,\eta]^T$ or $[x\,x_o]^T$)
η	Augmented error states
x_o	Observer states (e.g. $\left[\hat{x}\,\hat{\vartheta}\right]^T$ in Sec. 4.4.2)
x_{cl}	Plant, compensator, and exogenous states (e.g. $[x\,\eta\,\vartheta]^T$ in Sec. 2.2.1)
x_f	final state
Q, R	LQR design state and input weights
ξ	decoupled states (zero dynamics)

Appendix B. SAMPLE CODE

The following pages contain code samples as follows

1. Error Augmentation type regulator Sec. 2.2.1 (Matlab)
2. Disturbance Estimation type regulator Sec. 2.2.2 (Matlab)
3. Common Quadratic Lyapunov Function Sec. 4.2 (Matlab)
4. Multiple Model Adaptive Regulator Simulation Sec. 6.2 (Mathematica)

with details below in the order listed above.

Name	**regProcB.m**
Purpose	Obtain an Error Augmentation type regulator Eqn. (2.5)
Inputs	open loop plant matrices A, B, C or a State Space object $ss\,(A, B, C)$ Disturbance mapping matrices E, F Design weights J Internal Model Z
Outputs	state space object of controller with augmented states Eqn. (2.6) state space object with controller and disturbance states Eqn. (2.8) State Feedback gains Eqn. (2.7) (with fixed LQR gains)

Name	**regProcKB91.m**
Purpose	Obtain an Disturbance Estimation type regulator per [KK78], [KBB91]
Inputs	open loop plant matrices A, B, C or a State Space object $ss\,(A, B, C)$ Disturbance mapping matrices E, F Internal Model Z
Outputs	state space object of controller with estimation states state space object with controller and disturbance states Eqn. (4.20) Observer gain L such that Eqn. (4.21) holds (with fixed LQR gains) State Feedback gain K from Eqn. (2.10) (with fixed LQR gains) Lyapunov Matrix P for controller gains K Equilibrium solution for X, U from Eqn. (2.9)

Name	**commonGainRegSynthB.m**
Purpose	Obtain a CQLF for Error Augmentation regulation of a set of plants
Inputs	a cell array of State Space objects
Outputs	a Common Quadratic Lyapunov matrix P

Name	**MMAC Simulation**
Purpose	simulate continuous and discrete state MMAC in Mathematica
Inputs	a set of plants defined by substitution rules *subs* Disturbance mapping matrices E, F Design weights J Internal Model Z Controller Gains K_i, $i \in \{1, 2\}$
Outputs	Interpolating Functions *sols* and plots

Figure B.1: Matlab code for Error Augmentation type regulator (regProcB)

```
% given A,B,C,E,F and J,Z
% xDt = Ax + Bu + Ew
% wDt = Zw
%   e = Cx - Fw
%implement controller
% nDt = Zn + Je
function [sysC,sysCL,K] = regProcB(varargin) %regProcB(A,B,C,E,F,J,Z) vs regProcB(sys,E,F,J,Z)
if length(varargin)==7
    A = varargin{1}; B = varargin{2}; C = varargin{3}; E = varargin{4}; F = varargin{5};
    J = varargin{6}; Z = varargin{7};
elseif length(varargin)==5
    sys = varargin{1}; E = varargin{2}; F = varargin{3}; J = varargin{4}; Z = varargin{5};
    [A,B,C,D] = ssdata(sys);
else
    error('wrong number of input arguments')
end
%test for dimensional consistency, {m,n,p} = dim{u,x,y}, r is dim(Z)
[n,n2] = size(A); [n3,m] = size(B); [p,n4] = size(C);
[n5,r] = size(E); [p2,r2] = size(F); [r3,r4] = size(Z); [r5,p3] = size(J);

if any(n~=[n2 n3 n4 n5]), error('incorrect state dim'), end
if any(r~=[r2 r3 r4 r5/p]), error('incorrect dist dim'), end
if any(p~=[p2 p3]), error('incorrect output dim'), end
if m~=p, error('unbalanced # or controls or measurments'), end

Zs = []; for i=1:p, Zs = blkdiag(Zs,Z); end     %strong internal model
if rank(ctrb(Zs,J))<r*p, error('uncontrollable dist model'), end

% J is r x p, C is p x n
Ac = [A zeros(n,r*p);J*C Zs];   %Ac is (n+r,n+r)
Bc = [B; zeros(r*p,m)];         %Bc is (n+r,m)
Cc = [C, zeros(p,r*p)];         %Cc is (p,n+r*p)

[K,Sq,Eq] = lqr(Ac,Bc,eye(n+r*p),eye(m));

%Closed Loop System w/ Disturbance Model
As = [Ac-Bc*K [E;-J*F];zeros(r,n+r*p) Z];
Bs = [Bc; zeros(r,m)];
Cs = [C zeros(p,r*p) -F];

sysC = ss(Ac,Bc,Cc,0);
sysCL = ss(As,Bs,Cs,0);
```

Figure B.2: Matlab code for Disturbance Estimation type regulator (regProcKB91)

```
% Implement Regulator Design Procedure A Kwatny & Kalnitsky 78
% notation follows Kwatny Bennet Berg IEEE TAC 1991:
% given A,B,C,E,F,Z
% xDt = Ax + Ew+ Bu
% wDt = Zw
%   e = Cx + Fw
% sign change in "F" compared to regProcA & regProcB

function [sysC,sysCL,L,K,P,x] = regProcKB91(varargin) %regProcKB91(A,B,C,E,F,Z) vs regProcKB91(sys,E,F,Z)
if length(varargin)==6
    A = varargin{1}; B = varargin{2}; C = varargin{3}; E = varargin{4}; F = varargin{5}; Z = varargin{6};
elseif length(varargin)==4
    sys = varargin{1}; E = varargin{2}; F = varargin{3}; Z = varargin{4};
    [A,B,C,D] = ssdata(sys);
else
    error('wrong number of input arguments')
end

%test for dimensional consistency, {m,n,p} = dim{u,x,y}, r is dim(Z)
[n,n2] = size(A); [n3,m] = size(B); [p,n4] = size(C);
[n5,r] = size(E); [p2,r2] = size(F); [r3,r4] = size(Z);

if any(n~=[n2 n3 n4 n5]), error('incorrect state dim'), end
if any(r~=[r2 r3 r4]), error('incorrect dist dim'), end
if any(p~=[p2]), error('incorrect output dim'), end
if m~=p, error('unbalanced # or controls or measurments'), end

%Solve for translations
%A*T + B*V = -G (E)
%C*T       = -H (F)

%KB91 Section C, Step 1
M = [A B;C zeros(p,m)]; b = -[E; F]; x = inv(M)*b;
X = x(1:n,:); U = x(n+1:end,:);

%KB91 Section C, Step 2
[Km,P,eigsK] = lqr(A,B,eye(n),eye(m)); Ko=-Km; K = [Ko, U-Ko*X];

%KB91 Section C, Step 3
Av = [A E;zeros(r,n) Z]; Bv = [B; zeros(r,m)]; Cv = [C F];
[Lt,~,eigsL] = lqr(Av',Cv',eye(n+r),eye(m)); L=-Lt'; L1 = L(1:n,:); L2 = L(n+1:end,:);

% Closed Loop Dynamics
% default tune Q = I_r
Q = eye(p);
% xDt = Ax + Gw + Bu where u = U*v2 + Ko*(v1 - X*v2)
% v1Dt = (A + L1*C + B*Ko)*v1 + (G + L1*H + B*(U-Ko*X))*v2 - L1*Q*(y-y*);
% v2Dt = (L2*C)*v1 + L2*H*v2 -L1*Q*(y-y*);
% wDt = Zw
% %where y = Cx, y* = -Hw, states are xBar = [x v1 v2 w], xBarDt = As*xBar
% As =  [A               B*Ko         B*(U-Ko*X)          G     ]
%       [-L1*Q*C      A+L1*C+B*Ko   G+L1*H+B*(U-Ko*X)  L1*Q*-H  ]
%       [-L2*Q*C        L2*C           L2*H           L2*Q*-H  ]
%       [0                0              0              Z     ]

%Closed loop system matrices As, Bs, Cs
As = [A,B*Ko,B*(U-Ko*X),E;
     -L1*Q*C,A+L1*C+B*Ko, E+L1*F+B*(U-Ko*X),L1*Q*-F;
     -L2*Q*C, L2*C, L2*F, L2*Q*-F;
     zeros(r,n),zeros(r,n+r),Z];

Bs = [Bv; zeros(n+r,m)];
Cs = [C zeros(p,n+r) F];

sysCL = ss(As,Bs,Cs,0);

%Open Loop System w/ Disturbance Model
sysC = ss(Av,Bv,Cv,0);
```

Figure B.3: Matlab code to obtain a CQLF for the Error Augmentation regulator (commonGainRegSynthB)

```
% Input: cell array of lti sys objects with state vector xb = [x eta],
%          ie Ar = [A 0;JC Z], Br = [B;0], Cr = [C 0]
% Define: weights Cz,Dz
% Output: P such that Klmi = -inv(Dz'*Dz)*Br'*P,
%          (left to user since B may be f(theta))

function [P] = commonGainsRegSynthB(sysC,n)

[nPr,m]=size(sysC{1}.b); %assume square system, #inputs = #outputs, i.e. m = p
r = nPr - n;

Q=sdpvar(nPr,nPr,'symmetric');
F = set(Q>0);

%customize LQR tuning here
Qz = eye(nPr);     %regulator states are [x eta]
Rz = eye(m);

Cz = [Qz; zeros(m,nPr)];
Dz = [zeros(nPr,m); Rz];

ind = length(sysC);
for i=1:ind

    A = sysC{i}.a; B = sysC{i}.b;
    Y = -inv(Dz'*Dz)*B';

    X = blkvar; %form one LMI
    X(1,1) = A*Q+Q*A'+B*Y+Y'*B';
    X(1,2) = (Cz*Q+Dz*Y)';
    X(2,2) = -eye(nPr+m);
    X = sdpvar(X);

    F = F + set(X<0); %form block LMI

end

solvesdp(F,-geomean(Q));    %solve block LMI

P = inv(double(Q));         %unpack answer
```

Figure B.4: Mathematica code for MMAC simulation

```
(* Form closed loop regulator dynamics *)
(* Ai, Bi associate vertex ϑij with A(ϑij) & B(ϑij) *)
Clear[ACL]
ACL[subs_, E_, F_, Z_, J_, K_] := Module[{n, m, p, r, r2, Ac, Bc, Cc, Dc}, {
   {p, r2} = Dimensions[F], {n, r2} = Dimensions[E], m = p, {r, r} = Dimensions[Z],
   Ac = ArrayFlatten[{{Ai[subs], 0}, {J.C2, Z}}],
   Bc = ArrayFlatten[{{Bi[subs]}, {zeros[r, m]}}],
   Cc = ArrayFlatten[{{C2, 0}}],
   Dc = ArrayFlatten[{{E}, {-F}}]
  }; ArrayFlatten[{{Ac + Bc.K, Dc}, {0, zeros[r2]}}]] (* ϑDt=Z=0 *)

(* Dynamics ẋ=f(x,σ,t) *)
Clear[f]
f[ind_, x_, σ_, t_?NumericQ] := ACL[eqIndT, EvT, Fv, Z, J, Kv[[σ]]][[ind]].x /; t < 1
f[ind_, x_, σ_, t_?NumericQ] := ACL[eqIndB, EvB, Fv, Z, J, Kv[[σ]]][[ind]].x /; t ≥ 1

(* Switching Functions *)
Clear[evalLypFuncs, SwitchTable]
evalLypFuncs[x_, xPrev_, P_] := x.P.x < xPrev.P.xPrev;
(* Switch Table *)
SwitchTable[q_, bot_, top_, t_] := Module[{q0 = q}, {
    If[q = 1 && bot = False, {q0 = 2}],
    If[q = 2 && top = False, {q0 = 1}]};
   q0];
(* Switch Logic - Requires xf & P for Bottom and Top sheets *)
Clear[switchLogic, xOut, boolQ]
switchLogic[x_, q_, t_?NumericQ] := Module[{xP = xOut[[-1]], boolTop , boolBot}, {
    boolTop = evalLypFuncs[x - xFt, xP - xFt, Pt];
    boolBot = evalLypFuncs[x - xFb, xP - xFb, Pb];
    (* log xOut for use in V(t)<V(t-dT) *)
    xOut = Append[xOut, x], boolQ = Append[boolQ, {boolBot, boolTop}]};
   SwitchTable[q, boolBot, boolTop, t]];
(* WhenEvent Logic *)
Events = { WhenEvent[Mod[t, 1/1000] = 0, {σ[t] → switchLogic[{v[t], α[t], θ[t], q[t], η1[t], η2[t]}, σ[t], t]}] };

(* Equations of Motion *)
xOfT = Map[#[t] &, x8]; DxDt = Map[#'[t] &, x8];
stateEqns = Thread[DxDt == Table[f[i, xOfT, σ[t], t], {i, 8}]]; (* continous states *)
states = Join[x8, {σ}];
eqnsOfMotion = Join[stateEqns, InitialConds, Events];

(* Execute Simulation *)
InitialConds = {v[0] = 0.55, α[0] = 0.218824, θ[0] = 0.218824, q[0] = 0, η1[0] = 0, η2[0] = 0, ϑ1[0] = 0.5, ϑ2[0] = 0, σ[0] = 2};
xOut = {InitialConds[[ ;; 6, 2]]}; boolQ = {};
tEnd = 2;
sols = NDSolve[diffEq, states, {t, 0, tEnd}, DiscreteVariables → {σ},
   AccuracyGoal → 1, PrecisionGoal → 1,
   StartingStepSize → 1/1000, MaxSteps → 5000, Method → {"FixedStep", Method → "ExplicitEuler"}];

(* Verify *)
pX = Table[Plot[Evaluate[x8[[i]][t] /. sols], {t, 0, tEnd}, AxesLabel → {t, x8[[i]]}, PlotRange → All, PlotStyle → Red], {i, 8}]
```

Vita

Eric D. Peterson

Education

Drexel University, Philadelphia, PA

Ph.D., Mechanical Engineering and Mechanics — 2014

- Dissertation Topic: "Multiple Model Adaptive Regulation of Systems with Diverse Zero Structure"
- Advisor: Professor Harry Kwatny

Drexel University, Philadelphia, PA

M.S., Mechanical Engineering and Mechanics — 2003

LeTourneau University, Longview, TX

B.S., Engineering, Mechanical — 1999

Recent Publications

E. Peterson & H. Kwatny, *Multi-Model adaptive regulation for a family of systems containing different zero structures.* IFAC World Congress, Capetown, South Africa. Aug. 2014.

E. Peterson & H. Kwatny, *Multi-Model Adaptive Regulation for Aircraft Dynamics with Different Zero Structures.* ASME Dynamic Systems & Control Conf. San Antonio, Texas. Oct 2014.

Coursework

Candadicy Exams in Robust and Nonlinear Control

Teaching Assistant

MEM355/351 Dynamic Systems (Theory/Lab)
MEM667 Graduate Dynamics
ENGR180 Math Supplement for Engineers
MEM380 Special Topics: Autonomous Vehicle Lab

Professional Experience

General Dynamics Robotic Systems, Westminster, MD

Sr. Engineer — 2003 -2010
Guidance, Navigation, and Control of Autonomous Ground Vehicles

Boeing Rotorcraft, Ridley Park, PA

Engineer — 2000 -2003
Comanche Helicopter Avionics & Armament Integration